Title

IL-2 can signal via chemokine receptors to promote regulatory T cells' suppressive function

Journal

Cell Reports, 42(8)

ISSN

2639-1856

Authors

Sun, Hao
Lee, Ho-Sup
Kim, Sarah Hyun-Ji
et al.

Publication Date

2023-08-01

DOI

10.1016/j.celrep.2023.112996

Peer reviewed

Cell Reports

Article

IL-2 can signal via chemokine receptors to promote regulatory T cells' suppressive function

Graphical abstract

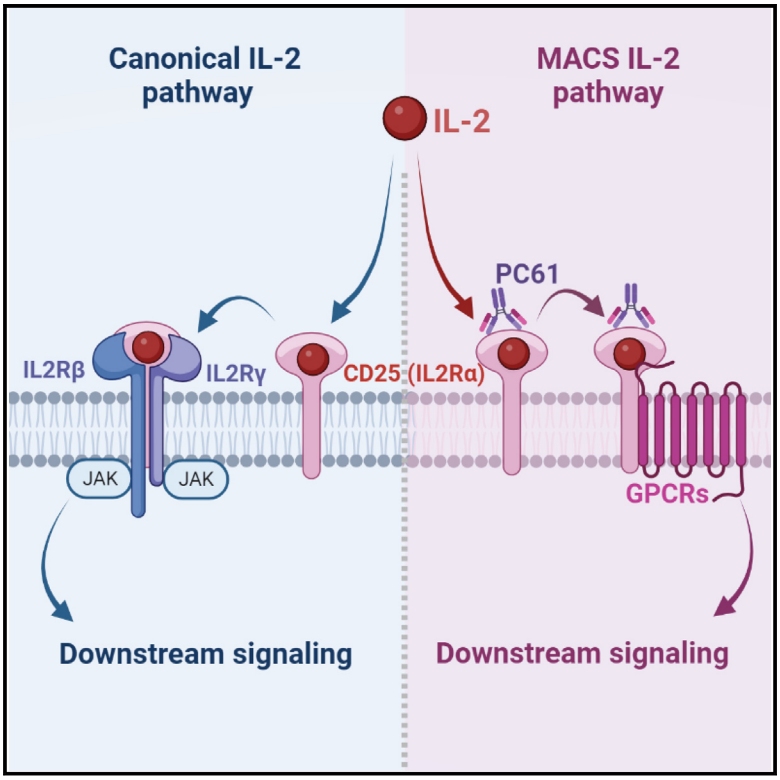

Authors

Hao Sun, Ho-Sup Lee, Sarah Hyun-Ji Kim, ..., Derek VanDyke, Jamie B. Spangler, Mark H. Ginsberg

Correspondence

mhginsberg@ucsd.edu

In brief

IL-2 shapes the immune response. Sun et al. report that IL-2 signaling via a CD25-chemokine receptor pathway promotes increased regulatory T cells' suppressive function. An anti-CD25 or heparan sulfate biases IL-2 signaling toward this chemokine receptor pathway, and administration of a modified form of this anti-CD25 ameliorates murine experimental autoimmune encephalomyelitis.

Highlights

- IL-2 can signal via chemokine receptors (CRs) in addition to the βγ IL-2 receptors
- An anti-CD25 induces a CD25-IL-2-CCR7 complex and enforces CR signaling
- This non-canonical IL-2 signaling pathway promotes Tregs' suppressive function
- A modified form of this anti-CD25 ameliorates experimental autoimmunity

Sun et al., 2023, Cell Reports *42*, 112996
August 29, 2023
https://doi.org/10.1016/j.celrep.2023.112996

CellPress

Cell Reports

CellPress
OPEN ACCESS

Article

IL-2 can signal via chemokine receptors to promote regulatory T cells' suppressive function

Hao Sun,[1] Ho-Sup Lee,[1] Sarah Hyun-Ji Kim,[1] Mikhael Fernandes de Lima,[1] Alexandre R. Gingras,[1] Qinyi Du,[1] Wilma McLaughlin,[1] Jailail Ablack,[1] Miguel A. Lopez-Ramirez,[1,7] Frederic Lagarrigue,[2] Zhichao Fan,[3] John T. Chang,[1] Derek VanDyke,[4] Jamie B. Spangler,[4,5,6] and Mark H. Ginsberg[1,8,*]

[1]University of California San Diego School of Medicine, La Jolla, CA, USA
[2]Institute of Pharmacology and Structural Biology, Toulouse, France
[3]University of Connecticut School of Medicine, Farmington, CT, USA
[4]Department of Chemical & Biomolecular Engineering, Johns Hopkins School of Medicine, Baltimore, MD, USA
[5]Department of Biomedical Engineering, Johns Hopkins School of Medicine, Baltimore, MD, USA
[6]Translational Tissue Engineering Center, Johns Hopkins School of Medicine, Baltimore, MD, USA
[7]Department of Pharmacology, University of California, San Diego, La Jolla, La Jolla, CA, USA
[8]Lead contact
*Correspondence: mhginsberg@ucsd.edu
https://doi.org/10.1016/j.celrep.2023.112996

SUMMARY

Canonical interleukin-2 (IL-2) signaling via the high-affinity CD25-containing IL-2 receptor-Janus kinase (JAK) 1,3-signal transducer and activator of transcription 5 (STAT5) pathway is essential for development and maintenance of $CD4^+CD25^{Hi}Foxp3^+$ regulatory T cells (Tregs) that support immune homeostasis. Here, we report that IL-2 signaling via an alternative CD25-chemokine receptor pathway promotes the suppressive function of Tregs. Using an antibody against CD25 that biases IL-2 signaling toward this alternative pathway, we establish that this pathway increases the suppressive activity of Tregs and ameliorates murine experimental autoimmune encephalomyelitis (EAE). Furthermore, heparan sulfate, an IL-2-binding element of cell surfaces and extracellular matrix, or an engineered IL-2 immunocytokine can also direct IL-2 signaling toward this alternative pathway. Overall, these data reveal a non-canonical mechanism for IL-2 signaling that promotes suppressive functions of Tregs, further elucidates how IL-2 supports immune homeostasis, and suggests approaches to promote or suppress Treg functions.

INTRODUCTION

Interleukin-2 (IL-2) is necessary for the expansion and maintenance of regulatory T cell (Treg) and conventional T cell (Tconv) subsets. Extensive research over more than 25 years has established the canonical IL-2 signaling pathway. IL-2 binds to the α receptor (CD25) favoring IL-2 association with the signaling β(CD122)γ(CD132) subunits, and the resulting high-affinity receptor activates associated Janus kinases (JAKs) 1 and 3, resulting in recruitment and phosphorylation of signal transducer and activator of transcription 5 (STAT5) in addition to other pathways such as PI3 kinase.[1] IL-2 plays a central role in the development of $CD4^+FOXP3^+CD25^{Hi}$ Tregs that maintain homeostasis by limiting immune responses.[2] Treg deficiency, instability, or dysfunction can contribute to autoimmunity.[3] Adoptive transfer of Tregs can delay or prevent graft rejection and control autoimmune responses.[4] Certain anti-IL-2 antibodies[5,6] or IL-2 muteins[7] bias IL-2 signaling to Tregs, thereby expanding endogenous Tregs and suppressing autoimmunity. Thus, increasing Treg abundance through the canonical IL-2 signaling pathway is an actively pursued tool for the prevention of transplant rejection and the treatment of autoimmune diseases.[8]

Integrin activation plays an important role in Tregs' suppressive function and migration.[9–11] Leukocyte integrins including αLβ2 (LFA-1, CD11a/CD18), α4β1 (VLA-4), and α4β7[12] are usually in a low-affinity state until agonist stimulation induces a high-affinity form, a process operationally defined as "integrin activation." Binding of talin to the cytoplasmic tail of integrins β1 and β3,[13] β2,[14] and β7[11] is a critical final common step in integrin activation. Rap1 GTPases are important signaling hubs that control integrin activation in blood cells.[15,16] Mice expressing an integrin activation-defective talin1 mutant, talin1(L325R), in Tregs developed autoimmunity resembling that due to inactivation of *Foxp3*, indicating that integrin activation is required for Treg function.[9,10] Conversely, an anti-β1 antibody that activates β1 integrins increases the suppressive capacity of talin1-deficient Tregs.[9] Rap1 and its effectors Rap-interacting adaptor molecule (RIAM; *Apbb1ip*) and Lamellipodin (Lpd; *Raph1*) are involved in Treg integrin activation and suppressor function.[10,17] Together, these data show that integrin activation plays a critical role in regulating Treg function and raises the possibility that enforcing Treg integrin activation may serve to amplify their suppressor function, thereby blunting immune responses.

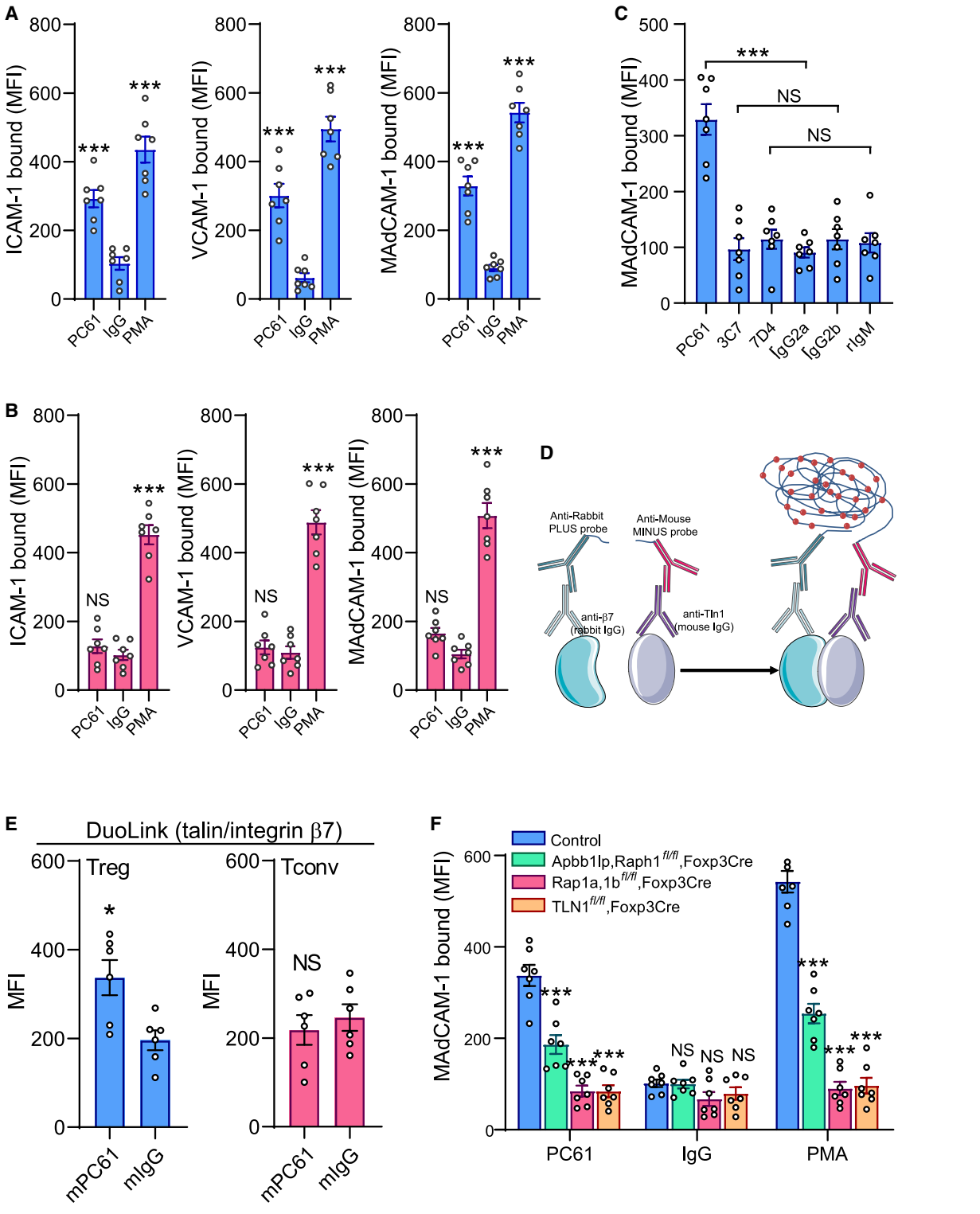

Figure 1. PC61 triggers integrin activation in Tregs

(A and B) Binding of soluble ICAM-1, VCAM-1, or MAdCAM-1 to CD4 T cells in the presence of PC61 (5 μg/mL) or PMA (100 nM). GFP$^+$ Tregs (A) or GFP$^-$ Tconvs (B) were analyzed. Data represent mean ± SEM (n = 7). One-way ANOVA with Bonferroni post-test.

(C) Binding of soluble MAdCAM-1 to GFP$^+$ Tregs in the presence of 5 μg/mL PC61, 7D4, or 3C7 was analyzed. Data represent mean ± SEM (n = 7). One-way ANOVA with Bonferroni post-test.

(legend continued on next page)

Antibodies against CD25 were developed to suppress Tconv proliferation[18]; however, such antibodies can induce paradoxical autoimmunity by suppressing Treg function.[19,20] Conversely, anti-CD25 antibodies, such as PC61, are used as an experimental tool to deplete Tregs.[21] Indeed, Treg-depleting antibodies have also been proposed as an adjuvant to cancer immunotherapy.[22] Here, we report that PC61, but not two other anti-CD25 antibodies, induce integrin activation in Tregs, but not Tconvs, and amplify Tregs' suppressive function. The increased suppressive function required the central relays of the integrin activation pathway, Rap1 and talin1. Surprisingly, PC61-stimulated integrin activation did not use the canonical IL-2 signaling pathway. Instead, PC61 induced formation of a receptor formed by the IL-2-dependent association of CD25 with CCR7. Rather than signaling via JAKs and STAT5, this alternative receptor induces Gαi/o-dependent integrin activation. Furthermore, blockade of Gαi/o signaling abolished the capacity of PC61 to promote Tregs' suppressive function, thereby establishing that this alternative IL-2 signaling pathway is responsible for increased suppressive activity. Sulfated glycosaminoglycans, such as heparan sulfate, serve to dock IL-2 at tissue sites[23] and can promote Tregs' suppressive function.[24,25] Heparan sulfate biased IL-2 signaling toward this Gαi-dependent pathway. To test whether activation of this alternative IL-2 signaling pathway could modulate autoimmunity, we engineered a recombinant murinized effector-incompetent PC61 (mPC61) that maintained its capacity to activate integrins and promote suppressor function but did not deplete Tregs *in vivo*. Administration of mPC61 ameliorated murine experimental autoimmune encephalomyelitis (EAE) by promoting the local enrichment of Tregs and their suppressive products in the spinal cord without inducing global Treg expansion. These studies establish that an alternative IL-2 signaling pathway triggered via a CD25-chemokine receptor complex promotes Tregs' suppressor function and can ameliorate EAE, a model autoimmune disease.

RESULTS

An anti-CD25 antibody triggers integrin activation in Tregs, not in Tconvs

We serendipitously noted that PC61, a rat anti-mouse CD25, induced Treg, but not Tconv, activation of multiple integrins as assessed by binding of soluble ligands for αLβ2 (ICAM-1), α4β1 (VCAM-1), or α4β7 (MAdCAM-1) (Figures 1A and 1B). In contrast, other anti-mouse CD25 antibodies, such as 3C7, which competitively blocks IL-2 binding,[26] and 7D4, did not induce integrin activation in Tregs (Figure 1C). The interaction of talin with the integrin β cytoplasmic domain is a final intracellular step in physiological integrin activation.[13] To assess whether PC61 induced integrin activation via this physiological pathway, we used proximity ligation to assess the interaction between talin1 and the integrin β7 subunit in primary untransfected T cells (Figure 1D). PC61, but not control immunoglobulin G (IgG), increased the proximity ligation signal in Tregs but not in Tconvs (Figure 1E). Conversely, PC61 failed to activate integrin α4β7 (Figure 1F), αLβ2, or α4β1 (Figure S1) in talin null Tregs. Rap1 is the primary signaling enzyme upstream of talin1 in T cells,[10,15] and PC61 did not activate α4β7 (Figure 1F) or αLβ2 and α4β1 (Figure S1) integrins in combined Rap1a and Rap1b null Tregs. Lpd (*Raph1*) and RIAM (*Apbb1ip*) are important Rap1 effectors that engage talin,[27] and combined deletion of these two effectors partially suppressed the activation of Treg integrin α4β7 (Figure 1F) or αLβ2 and α4β1 (Figure S1) by PC61. Thus, PC61, but not several other anti-CD25 antibodies, triggers activation of Treg β1, β2, and β7 integrins by inducing Rap1-RIAM/Lpd-mediated talin-dependent integrin activation in Tregs.

PC61 enhances Tregs' suppressive function

We hypothesized that PC61, by activating Treg integrins, could enhance suppressive function. We added varying ratios of congenic Tregs (CD45.2$^+$) to carboxy fluorescein (CFSE)-labeled Tconvs (CD45.1$^+$ responder cells) and cultured them in the presence of 5 μg/mL PC61 or IgG. Tregs' suppressive activity was measured by reduction of the division of the responder cells. As expected, Tregs suppressed the division of responder cells in a dose-dependent manner; suppressive activity was dramatically enhanced by PC61 (Figure 2A). Importantly, PC61 had a negligible effect on the proliferation of the responder cells in the absence of added Tregs (Treg:responder ratio of 0 in Figure 2A). In the example shown, in the presence of PC61, ∼8 times fewer Tregs were required to generate the same degree of suppression as Tregs cultured with control IgG. This increased suppressive activity was tied to integrin activation because PC61 did not increase the negligible suppressive activity of Rap1a and Rap1b null Tregs (Figure 2A) that fail to activate integrins in response to PC61.

In the foregoing experiments, PC61 was incubated with Tregs and responder cells, and previous work has suggested that PC61 could favor the expansion of Tregs over Tconvs by suppressing IL-2 signaling in Tconvs.[28] Nevertheless, in our experiments, increased suppression was not associated with an increase in the number of Tregs in the cultures, and PC61 had little effect on responder cell proliferation in the absence of Tregs (Figure 2A). To directly assess whether PC61 was acting on the Tregs, Tregs were pre-incubated with PC61 and washed prior to co-culture with responder cells. PC61-treated cells showed ∼4-fold enhanced suppressive activity in comparison with Tregs

(D and E) The DuoLink proximity ligation assay was performed to measure the association of integrin β7 with talin1 in Tregs after PC61 stimulation.
(D) Schematic illustration of the DuoLink proximity ligation assay.
(E) CD4$^+$ T cells were stimulated with PC61 or IgG in 37°C for 30 min, fixed, permeabilized, and stained with rabbit anti-β7 and mouse anti-talin, and proximity ligation assay was performed to assess the interaction between integrin β7 and talin1. GFP$^+$ Tregs and GFP$^-$ Tconvs were analyzed. Data represent mean ± SEM (n = 6). Two-tailed t test.
(F) Binding of soluble MAdCAM-1 to Tregs from indicated gene-edited mice in the presence of PC61 (5 μg/mL) or PMA (100 nM). Data represent mean ± SEM (n = 7). One-way ANOVA with Bonferroni post-test. NS, not significant; **p < 0.01; ***p < 0.001.

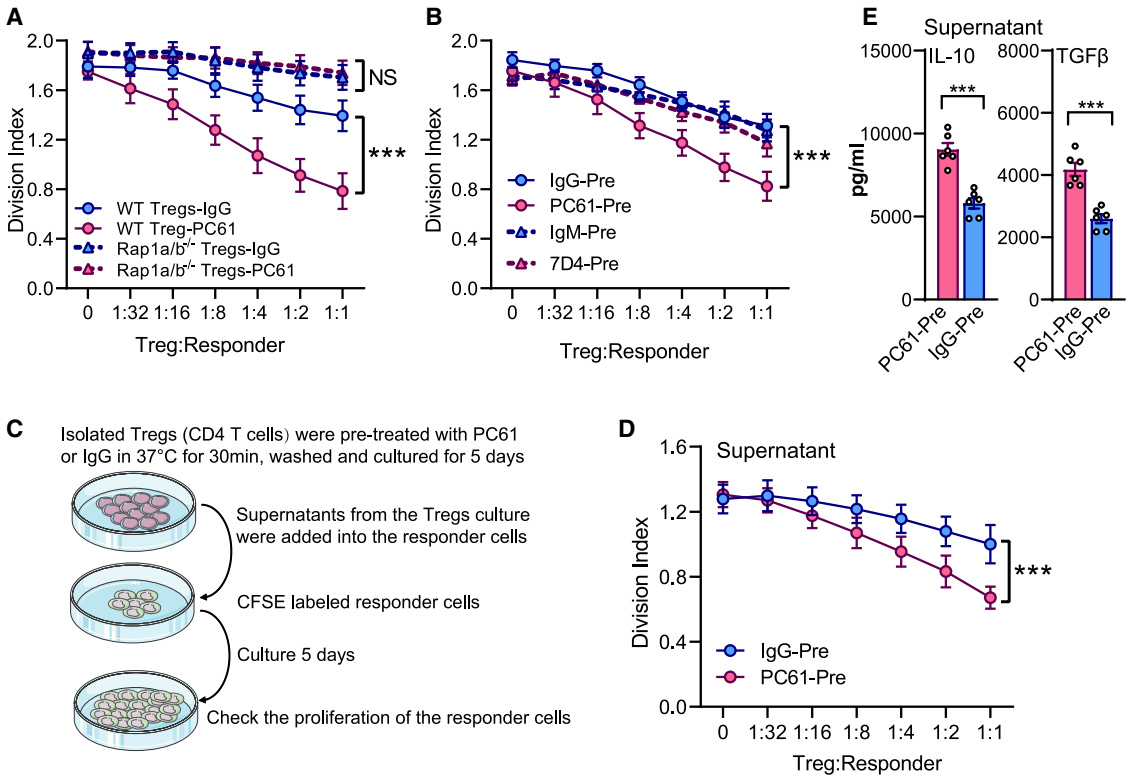

Figure 2. PC61 enhances Tregs' suppressive function and increases the secretion of IL-10 and TGF-β

(A and B) Tregs' suppressive activity.

(A) Tregs isolated from CD45.2 congenic *Rap1a*$^{fl/fl}$,*Rap1b*$^{fl/fl}$,*Foxp3*$^{YFP-Cre}$ mice (*Rap1a/b*^{TRKO}) or *Foxp3*^{GFP} mice were mixed with responder cells at the indicated Treg/responder cell ratios with either PC61 or IgG control treatment.

(B) Tregs isolated from CD45.2 congenic *Foxp3*^{GFP} mice were pre-incubated with either PC61 (PC61-Pre) or 7D4 (7D4-Pre) in 37°C for 30 min, washed, and then mixed with responder cells at the indicated Treg/responder cell ratios. Responder cells are CFSE-labeled CD45.1 congenic C57BL/6 CD4$^+$CD25$^-$ naive T cells activated by anti-CD3 (5 μg/mL), anti-CD28 (5 μg/mL), and IL-2. CFSE populations gated on CD45.1$^+$ cells were analyzed by flow cytometry on day 5 to determine the division index using FlowJo software. Data represent mean ± SEM (n = 9 in A or 6 in B). Two-way ANOVA with Bonferroni post-test.

(C and D) Isolated CD4 T cells were treated with PC61 or IgG for 30 min at 37°C, washed, and cultured for 5 days in complete RPMI 1640 medium with 0.6 ng/mL IL-2. Supernatants were collected and added into CFSE-labeled responder cells with anti-CD3 (5 μg/mL), anti-CD28 (5 μg/mL), and IL-2 (6 ng/mL). CFSE populations gated on CD45.1$^+$ cells were analyzed by flow cytometry on day 5 to determine the division index using FlowJo software. Data represent mean ± SEM (n = 6). Two-way ANOVA with Bonferroni post-test.

(E) The production of IL-10 and TGF-β from the supernatants of PC61 pre-treated CD4 T cells (in C and D) were determined by ELISA. Data represent mean ± SEM (n = 6). Two-way ANOVA with Bonferroni post-test. NS, not significant; *p < 0.05; **p < 0.01; ***p < 0.001.

pre-treated with IgG control or with another anti-CD25 antibody, 7D4 (Figure 2B). The reduction in PC61 enhancement of suppression on pre-treated Tregs relative to an assay (Figure 2A) conducted in the continuous presence of free PC61 is ascribable to synthesis of PC61-free CD25 during the 5-day incubation. To better understand the mechanism of action of PC61, we tested the effect of PC61 stimulation on expression of suppressive cytokines. The supernatant from the PC61-pre-treated Treg cultures suppressed the division of responder cells cultured in the absence of Tregs (Figures 2C and 2D). Furthermore, the supernatant from PC61-pre-treated Tregs contained more of the suppressive Treg products IL-10 and transforming growth factor β (TGF-β) (Figure 2E), suggesting that PC61 enhances Tregs' suppressive function in part by stimulating the secretion of IL-10 and TGF-β, although many other potential mechanisms of suppression exist.[29]

PC61 does not activate the canonical IL-2 signaling pathway

CD25 (IL-2Rα) participates in canonical IL-2 signaling[1] by binding to IL-2, resulting in IL-2 recruitment to IL-2Rβ (CD122) and IL-2Rγ (CD132) to form a quaternary complex. Complex formation activates JAK1 and JAK3, which in turn leads to phosphorylation of STAT5. TM-β1, which blocks IL-2 canonical signaling by interfering with IL-2 binding to IL-2Rβ (CD122),[30] did not block PC61-induced integrin activation. In contrast, high-dose-IL-2-induced activation was abolished by TM-β1 (Figure 3A). Furthermore, PC61 failed to induce STAT5 phosphorylation in Tregs, in sharp contrast to IL-2 (Figure 3B). Similarly, 100 nM baricitinib, a JAK inhibitor, did not reduce PC61-induced integrin activation, although it markedly suppressed IL-2-induced STAT5 phosphorylation (Figures 3C and 3D). In sum, PC61 activated Treg integrins and enhanced suppressive function in a manner dependent on Rap1-RIAM/LPD-talin1

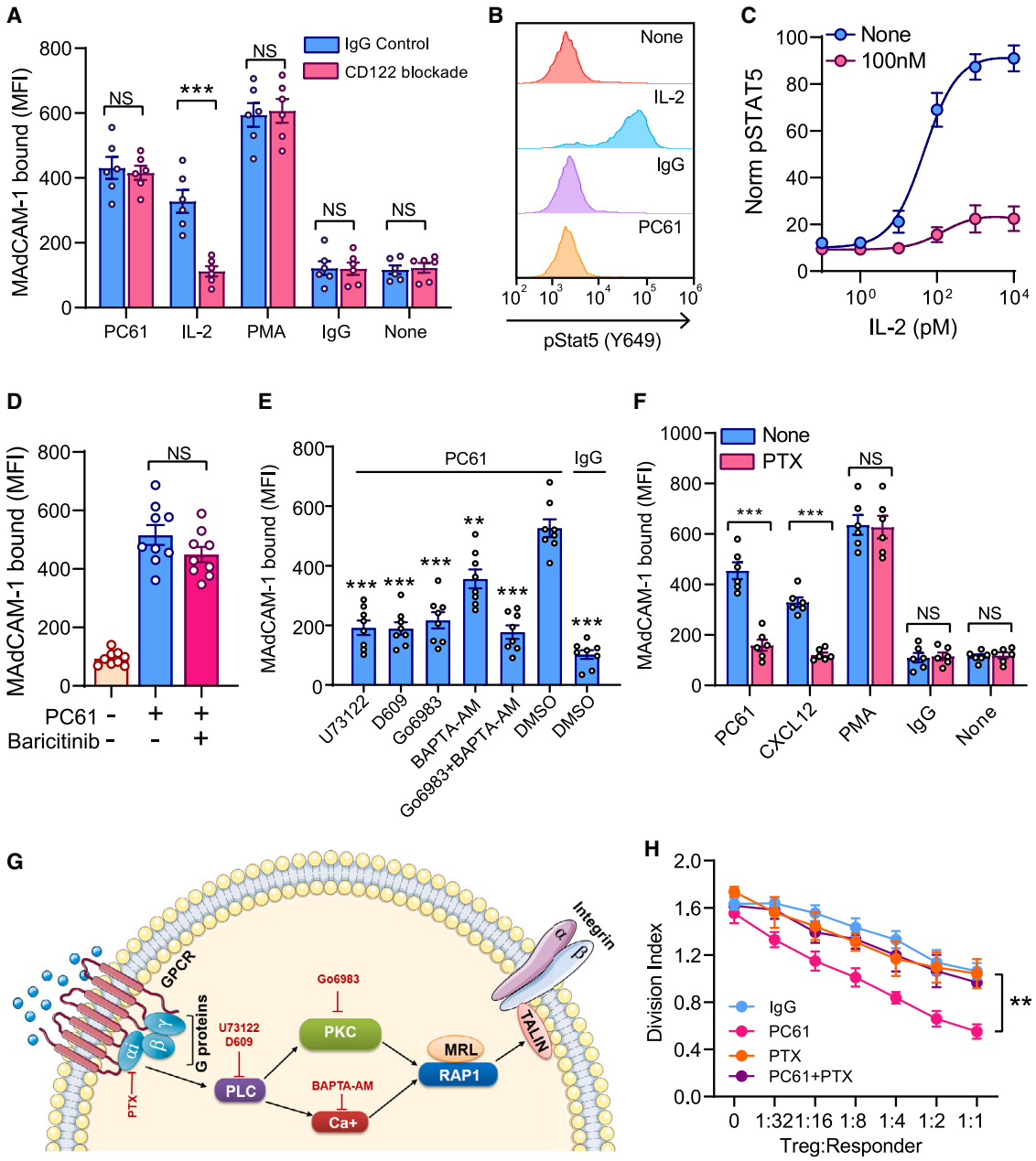

Figure 3. PC61 binding to CD25 activates Treg integrins via an alternative signaling pathway

(A) Binding of soluble MAdCAM-1 to CD4 T cells treated in the presence or absence of inhibitory anti-IL-2 receptor β (TMB1) with PC61 (5 μg/mL), IL-2 (2.5 μg/mL), or PMA (100 nM). GFP$^+$ Tregs were analyzed. Data represent mean ± SEM (n = 6). One-way ANOVA with Bonferroni post-test. NS, not significant; ***p < 0.001.

(B) STAT5 phosphorylation of CD4 T cells in the presence of PC61 (5 μg/mL) or IL-2 (2.5 μg/mL). GFP$^+$ Tregs were analyzed. Data are representative of at least three independent experiments.

(C) STAT5 phosphorylation response of GFP$^+$ Tregs to IL-2 in the presence or absence of 100 nM baricitinib. Data represent mean ± SEM (n = 6).

(D) Binding of soluble MAdCAM-1 to GFP$^+$ Tregs treated with 5 μg/mL control IgG (–) or PC61. The addition of 100 nM baricitinib did not significantly affect the response to PC61. Data represent mean ± SEM (n = 9). One-way ANOVA with Bonferroni post-test. NS, not significant.

(E) Binding of soluble MAdCAM-1 to CD4 T cells treated with indicated inhibitors in the presence of PC61 (5 μg/mL) or IgG control. GFP$^+$ Tregs were analyzed. Data represent mean ± SEM (n = 6). One-way ANOVA with Bonferroni post-test.

(F) Binding of soluble MAdCAM-1 to CD4 T cells treated with pertussis toxin (PTX) (100 nM) or vehicle in the presence of PC61 (5 μg/mL), CXCL12 (1 μg/mL), or PMA (100 nM). GFP$^+$ Tregs were analyzed. Data represent mean ± SEM (n = 6). One-way ANOVA with Bonferroni post-test.

(G) The key signaling events that occur downstream of GPCR signaling that lead to integrin activation.

(legend continued on next page)

intracellular signaling; however, this response was not dependent on the canonical IL-2 signaling pathway.

G protein-coupled receptor (GPCR) signaling mediates PC61-induced Treg integrin activation

To elucidate this non-canonical IL-2 signaling pathway, we assessed the effect of several kinase inhibitors on PC61-induced MAdCAM-1 binding to Tregs. U73122 and D609,[31,32] both of which target phospholipase C (PLC) nearly completely blocked PC61-induced integrin activation (Figure 3E). The principal products of PLC hydrolysis of PIP2 are di-acyl glycerol, which activates protein kinase C, and inositol triphosphate, which causes calcium release from intracellular stores. PC61-induced integrin activation was reduced when Tregs were treated with protein kinase C (PKC) inhibitor Go6983[33] or an intracellular Ca^{2+} chelator,[34] BAPTA-AM (N,N'-[1,2-ethanediylbis(oxy-2,1-phenylene)]bis[N-[2-[(acetyloxy)methoxy]-2-oxoethyl]-1,1'-bis[(acetyloxy)methyl] esterglycine). Furthermore, the combination of Go6983 and BAPTA-AM inhibited integrin activation to a similar degree as the PLC inhibitors (Figure 3E). PLC β is a primary target of Gαi-mediated signaling downstream of chemokine receptors,[35] pointing to the possible involvement of these receptors. To test this idea, pertussis toxin (PTX) was used to ADP ribosylate and inhibit Gαi/o.[36] PC61-mediated integrin activation in Tregs was blocked by PTX, as was the effect of a chemokine, CXCL12. Receptor-independent activation induced by phorbol myristate acetate was not inhibited by PTX, confirming the specificity of inhibition (Figure 3F). In sum, PC61 induces Treg integrin activation via Gαi/o-mediated activation of PLC, resulting in Rap1-RIAM/Lpd (MRL)-talin-dependent integrin activation in Tregs (Figure 3G).

We exploited the capacity of PTX to block PC61-induced integrin activation to interrogate the role of this alternative IL-2 signaling pathway in the capacity of PC61 to promote Tregs' suppressive function. Addition of PTX completely reversed the PC61-induced increase in Treg-mediated suppressive function (Figure 3H). This inhibitory effect of PTX was specific to the PC61-induced increased suppression because it had little effect on basal Tregs' suppressive activity in the absence of PC61. Thus, PC61 triggers a Gαi/o-dependent signaling pathway in Tregs, resulting in enhanced suppressive function.

PC61 stimulation triggers CCR7 association with CD25 in Tregs

Gαi/o plays a critical role in chemokine receptor signaling, and splenic Tregs express CCR4, CCR7, CCR8, CCR10, CXCR3, CXCR4, and CXCR5.[37] Among them, CCR7 is the most abundant chemokine receptor mRNA in naive murine splenic Tregs (Figure 4A; Skyline data: http://rstats.immgen.org/Skyline/skyline.html). To learn whether CCR7 is involved in PC61-stimulated integrin activation, we generated a human Jurkat T cell line that stably expresses mouse CD25 (mCD25-Jurkat) (Figure S2A) without affecting integrin β1 and β2 expression (Figure S2B). As previously observed with Tregs, PC61 was able to increase mCD25-Jurkat binding to VCAM-1, and this binding could be blocked by PTX (Figure S2C). However, the parental Jurkat cells were not stimulated by PC61, as they do not express mouse CD25 (Figure S2C). Importantly, these cells lacked detectable cell surface CD122 (Figure S2D) and did not manifest increased STAT5 phosphorylation in response to IL-2 (Figure S2E), thereby confirming that PC61-induced integrin activation occurs in the absence of the canonical IL-2 signaling pathway. CCR7 small interfering RNA (siRNA) was transfected into mCD25-Jurkat cells by electroporation, and CCR7 expression was reduced, while CXCR4 expression was unaffected (Figure S2D). Silencing CCR7 reduced the capacity of PC61 to promote mCD25-Jurkat cell integrin activation (Figure 4B), as did silencing CXCR4. Importantly, silencing CCR7 or CXCR4 blocked activation triggered by only their cognate cytokine ligands, CCL21 or CXCL12, respectively (Figure 4B). Silencing both CXCR4 and CCR7 together nearly completely blocked PC61-induced activation. Thus, PC61 stimulates integrin activation in mCD25-Jurkat cells via either CCR7 or CXCR4.

We speculated that PC61-CD25 might physically associate with CCR7 to stimulate integrin activation. To test this hypothesis, we used an immunoprecipitation (IP) blot approach where mCD25-Jurkat cells were stimulated with PC61 or 3C7 for 30 min, the cells were then lysed and mCD25 was affinity purified (Figure 4C), and the captured proteins were immunoblotted for the presence of CCR7; we were unable to obtain an immunoblotting antibody for CXCR4. CCR7 was co-isolated with CD25 when the cells were stimulated with PC61 but not when they were stimulated with 3C7 (Figure 4D). Thus, PC61 induced a physical association between CCR7 and CD25. Addition of PTX inhibited the PC61-induced association between CCR7 and CD25 (Figure 4D), indicating that functional Gαi/o is required for this association. CD25 was captured to the same extent in the presence or absence of PTX or 3C7.

To investigate whether PC61 induced the association between CCR7 and CD25 in primary Tregs, we performed a proximity ligation assay (Figure 4E). Due to the lack of commercial anti-Rat proximity ligation probes, we generated a mPC61 by exchanging the light- and heavy-chain Fv regions of rat PC61 (rPC61) with those of a murine IgG1. A heavy-chain D265A mutation was introduced to abolish FcγR binding[38] (Figure S3A). This murinized effector-incompetent PC61 (mPC61) bound Tregs with similar affinity and induced similar increases in integrin activation and suppressor function as the parent rat antibody (Figures S3B–S3E). $CD4^+$ T cells were treated with PC61 alone or in combination with PTX, fixed, and then stained with rabbit anti-CCR7 to label CCR7 in either YFP^+ Tregs or YFP^- Tconvs. We observed a significant increase in proximity ligation signal between CD25 and CCR7 in Tregs stimulated with mPC61 but not in Tconvs, and this interaction was inhibited by PTX (Figure 4F). Thus, CCR7 mediates PC61-induced integrin activation and can form a complex with CD25 in primary Tregs.

(H) PTX blocks PC61 enhancement of Tregs' suppressive activity. Tregs isolated from CD45.2 congenic *Foxp3*^{GFP} mice were mixed with responder cells at the indicated Treg/responder cell ratios in the presence of PC61 (5 μg/mL), PTX (100 nM), or PC61 together with PTX. Responder cells were CFSE-labeled CD45.1 congenic C57BL/6 $CD4^+CD25^-$ naive T cells activated by anti-CD3 (5 μg/mL), anti-CD28 (5 μg/mL), and IL-2 (6 ng/mL). CFSE populations gated on $CD45.1^+$ cells were analyzed by flow cytometry on day 5 to determine the division index using FlowJo software. Data represent mean ± SEM (n = 4). Two-way ANOVA with Bonferroni post-test. NS, not significant; $^{**}p < 0.01$; $^{***}p < 0.001$.

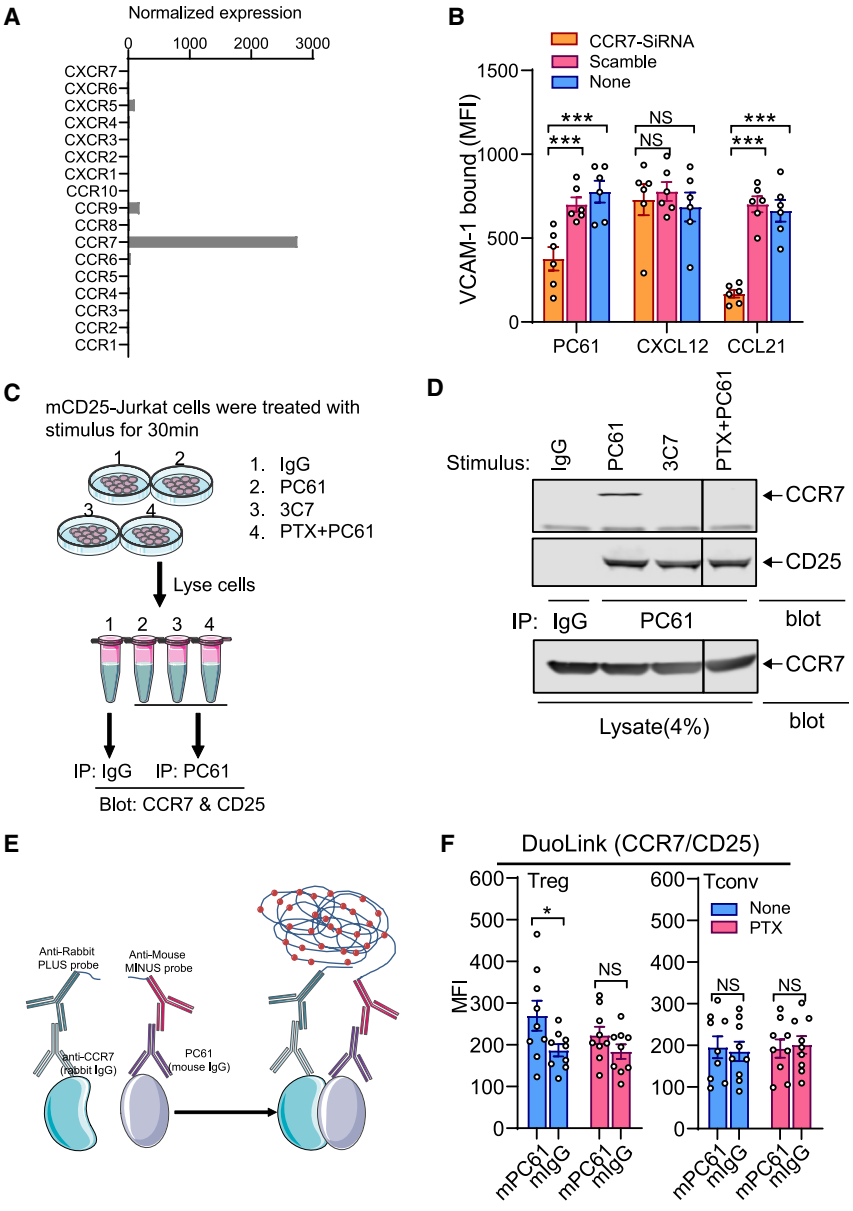

Figure 4. PC61 stimulation triggers CCR7 association with CD25

(A) The RNA expression level of chemokine receptors in murine splenic Tregs (http://rstats.immgen.org/Skyline/skyline.html).

(B) Jurkat cells stably expressing mouse CD25 (mCD25-Jurkat) were transfected with CCR7 or CXCR4 siRNA or scrambled-siRNA (2 μM) by Amaxa Nucleofector. 72 h post-transfection, the cells were stimulated with PC61 (5 μg/mL), CXCL12 (1 μg/mL), or CCL21 (1 μg/mL), and binding to soluble VCAM-1 was measured.

(C and D) Co-immunoprecipitation of CCR7 with CD25 after PC61 stimulation.

(C) Experimental scheme.

(D) Jurkat cells stably expressing mouse CD25 (mCD25-Jurkat) were treated with IgG control, PC61 (5 μg/mL), 3C7 (5 μg/mL), or PC61 combined with PTX (100 nM) at 37°C for 30 min and lysed. CD25 was isolated by immunoprecipitation (IP). CCR7 was analyzed by western blotting. Data are representative of at least three independent experiments. The PTX-treated cells were analyzed on the same SDS-PAGE as other samples; however, irrelevant intervening lanes were excised.

(E and F) The DuoLink proximity ligation assay was performed to measure the association of CCR7 with CD25 in primary untransfected Tregs after PC61 stimulation.

(E) Schematic illustration of the DuoLink proximity ligation assay.

(F) CD4 T cells were stimulated with murinized PC61 (mPC61) or mIgG at 37°C for 30 min in the presence or absence of PTX and then were fixed, permeabilized, and stained with rabbit anti-CCR7, and a proximity ligation assay was performed to assess the interaction between CCR7 and CD25. GFP$^+$ Tregs (left) and GFP$^-$ Tconvs (right) were analyzed. Data represent mean ± SEM (n = 9). One-way ANOVA with Bonferroni post-test. NS, not significant; *p < 0.05; **p < 0.01; ***p < 0.001.

PC61-mediated integrin activation in Tregs requires IL-2

In the foregoing experiments, we incubated PC61 with Tregs as part of a freshly isolated CD4$^+$ cell population. Surprisingly, when we used thrice-washed cells, we noticed a dramatic reduction in PC61-induced MAdCAM1 binding. Addition of 1.25 μg/mL IL-2 restored the PC61 response (Figure 5A). To investigate the potential role of IL-2 in PC61-induced integrin activation, we examined the effect of 3C7, an antibody known to directly compete for IL-2, but not PC61, binding to CD25.[21] PC61-stimulated MAdCAM-1-binding was blocked by 3C7 (Figure 5B), suggesting that IL-2 binding to CD25 is required. In contrast, the non-IL-2-blocking antibody 7D4 did not affect MAdCAM-1 binding (Figure 5B). The IL-2 neutralizing antibody (JES6-5H4, IL-2 Neut) blocks IL-2 binding to CD25,[39] and we found that IL-2 Neut also blocked PC61-stimulated integrin activation in Tregs (Figure 5C).

As noted above (Figure 4D), PC61 induces association of CD25 and CCR7 in Jurkat cells. To directly test the role of IL-2 binding to CD25, we generated a structure-based mouse CD25(R57E,V62E) mutant (mCD25(2E)), predicted to block IL-2 binding due to charge repulsion with IL-2 (Figure 5D). mCD25 wild-type or mCD25(2E) was expressed in HEK 293T cells, and the cells were stimulated with PC61, PC61 plus IL-2, or 3C7 plus IL-2. The cells were then lysed, CD25 was immunocaptured, and the presence of CCR7 was detected by immunoblotting (Figure S4A). PC61 induced association of CCR7 and mCD25 only in the presence of added IL-2 (Figure 5E). PC61 alone did not trigger the interaction because, unlike some Jurkat T cells,[40] HEK 293T cells do not secrete IL-2. Importantly, the structure-based CD25(2E) mutant did not form a complex with CCR7 in the presence of PC61 and IL-2 (Figure 5E), substantiating that the interaction between CD25 and CCR7 requires IL-2 binding

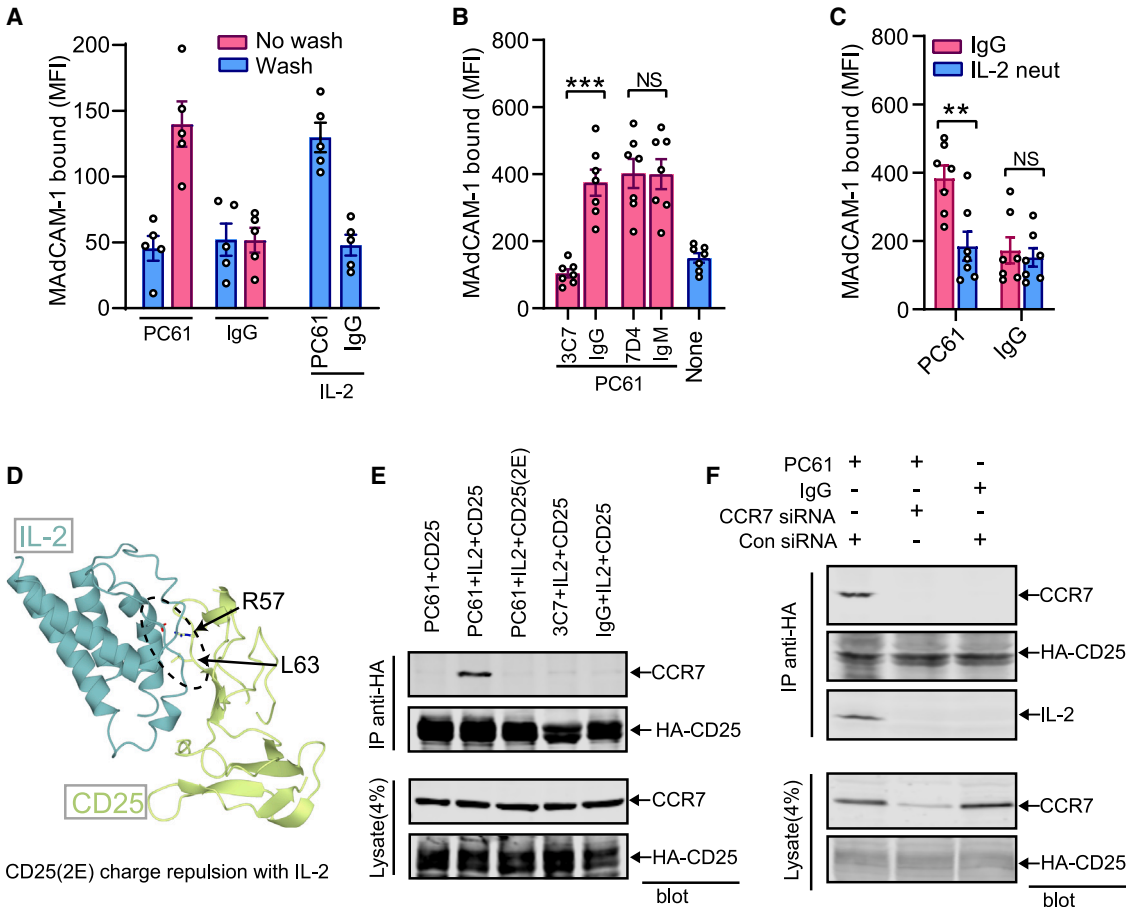

Figure 5. PC61-induced integrin activation requires IL-2

(A) Binding of soluble MAdCAM-1 to thrice-washed (Wash) or unwashed (No wash) CD4$^+$ T cells following addition of PC61 (5 μg/mL) in the presence or absence of 1.25 μg/mL IL-2. Data for GFP$^+$ Tregs are depicted and represent mean ± SEM (n = 5). One-way ANOVA with Bonferroni post-test.

(B) CD4$^+$ T cells were pre-treated with 5 μg/mL 7D4, 3C7, or Ig controls before addition of PC61 (5 μg/mL). Binding of soluble MAdCAM-1 to GFP$^+$ Tregs is depicted. Data represent mean ± SEM (n = 7). One-way ANOVA with Bonferroni post-test.

(C) CD4$^+$ T cells were stimulated with PC61 (5 μg/mL) or IgG control in the presence or absence of an antibody that blocks IL-2 binding to CD25 (IL-2 Neut) (2 μg/mL), and MAdCAM-1 binding to GFP$^+$ Tregs was measured. Data represent mean ± SEM (n = 7). One-way ANOVA with Bonferroni post-test.

(D) Structural model of the association of IL-2 and murine CD25. R57 and L63 are predicted to mediate interactions between IL-2 and CD25.

(E) IL-2 binding to CD25 is required for PC61-induced association of Cd25 with CCR7. 293T cells stably expressing hemagglutinin (HA)-tagged mouse CD25 or CD25(R57.L63E) (CD25(2E)) were treated with PC61 (5 μg/mL), PC61 plus IL-2 (5 μg/mL), 3C7 plus IL-2, or IL-2 alone at 37°C for 30 min and lysed. HA-CD25 and HA-CD25(2E) were captured by IP with anti-HA antibody. CCR7 was detected by immunoblotting. Data are representative of at least three independent experiments.

(F) CCR7 is required for the association of IL-2 with PC61-bound CD25. 293T cells stably expressing HA-tagged mouse CD25 were transfected with siRNA against CCR7 or control siRNA and after 48 h were incubated at 37°C for 30 min in the presence of IL-2 (2.5 μg/mL) and PC61 (5 μg/mL) or control IgG. Following lysis, HA-CD25 was captured by IP, and the presence of IL-2, CCR7, and CD25 was ascertained by immunoblotting. Data are representative of three independent experiments.

to CD25. Furthermore, immunoblotting showed that IL-2 was present in the PC61-induced CD25-CCR7 complex (Figure 5F) but was absent when CCR7 was silenced. Thus, IL-2 is required for PC61-induced integrin activation in Tregs and for the PC61-induced physical association of CD25 and CCR7.

Heparan sulfate or immunocytokines direct IL-2 signaling toward the non-canonical pathway

As shown above, PC61 binding to CD25 triggered IL-2-induced integrin activation via Gαi/o-dependent alternative pathway distinct from the canonical IL-2 signaling pathway. *In vivo*, IL-2 in tissues is bound to extracellular matrix heparan sulfate (HS), glycosaminoglycans. HS, heparin, or HS mimetics can promote the expansion, stability, or function of Tregs.[24,25,41] We therefore examined the effects of HS/IL-2 on Treg α4β7 integrin activation by measuring MAdCAM-1 binding. HS amplified IL-2 (2.5 μg/mL)-induced integrin activation in Tregs but not in Tconvs (Figure 6A, left panel, and S4B). Tregs harboring the talin1(L325R) mutation, which blocks the final step in integrin activation,[42] did not manifest increased integrin activation in

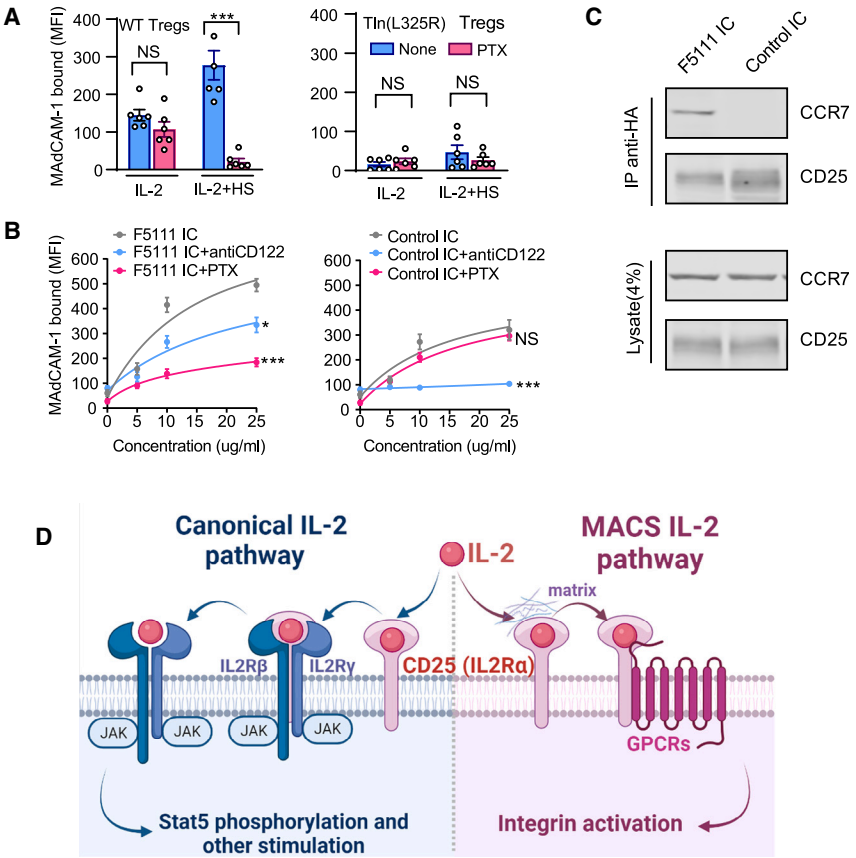

Figure 6. Heparan sulfate (HS) or an IL-2 immunocytokine bias IL-2 signaling toward the non-canonical pathway

(A) Binding of soluble MAdCAM-1 to YFP$^+$ Tregs isolated from either *Tln*$^{WT/fl}$;*Foxp3*$^{Cre\text{-}YFP}$ control mice or *Tln*$^{L325\ R/fl}$;*Foxp3*$^{Cre\text{-}YFP}$ mice treated with IL-2 (2.5 μg/mL) alone or in combination with HS (40 μg/mL) in the presence or absence of PTX (100 nM). Data represent mean ± SEM (n = 5). One-way ANOVA with Bonferroni post-test.

(B) Binding of soluble MAdCAM-1 to GFP$^+$ Tregs in the presence of either an F5111 immunocytokine (F5111 IC) or control anti-FITC IC (control IC) in the presence or absence of PTX or a function-blocking anti-IL-2 β receptor (anti-CD122). Data represent mean ± SEM (n = 6). Two-way ANOVA with Bonferroni post-test.

(C) F5111 IC induces association of human CD25 and CCR7.

(D) Extracellular matrix or monoclonal antibodies (e.g., PC61 or F5111) (depicted) can bias IL-2 signaling toward a chemokine receptor pathway. NS, not significant; *p < 0.05; **p < 0.01; ***p < 0.001.

response to either IL-2 or HS/IL-2 (Figure 6A, right panel), confirming that HS/IL-2 utilized the intracellular integrin activation pathway. HS/IL-2-induced activation was strongly inhibited by PTX, indicating that the capacity of HS/IL2 complexes to stimulate integrin activation is Gαi/o dependent. Thus, HS can bias IL-2 signaling toward this alternative pathway (Figure 6A).

The fact that HS can direct IL-2 signaling toward a Gαi/o-dependent pathway raises the possibility that manipulation of IL-2 by pre-complexing the cytokine with another molecule, such as an antibody, might also skew toward activation of this alternative pathway. Previous studies have shown that certain anti-IL-2 antibodies bias the cytokine toward activation of Tregs over immune effector cells by modifying cytokine-receptor interactions.[5,6,43] Biased engagement of Tregs can also be achieved by linking IL-2 to biasing anti-IL-2 antibodies, forming a single-chain fusion protein known as an immunocytokine (IC).[44,45] We therefore sought to explore the signaling properties of a Treg-biased IC (denoted F5111 IC) composed of human IL-2 linked to the anti-human IL-2 antibody F5111 via a $(Gly_4Ser)_7$ linker. F5111 blocks cytokine engagement of the βγ IL-2 receptor and allosterically impairs the cytokine's affinity for CD25.[6,45] We observed that the F5111 IC activated Tregs' integrins (Figure 6B, left panel). A control IC construct formed by linking IL-2 to an anti-FITC isotype control antibody also induced Tregs' integrin activation, albeit to a lesser extent (Figure 6B, right panel). PTX treatment markedly blocked integrin activation by the F5111 IC, whereas it had little effect on the control IC, indicating that F5111 IC was indeed engaging the alternative IL-2 signaling pathway (Figure 6B). In sharp contrast, the anti-CD122-blocking antibody TM-β1 abolished activation by the control IC while having a lesser effect on F5111 IC (Figure 6B). Thus, the control IC signals to integrins predominantly through the canonical IL-2 receptor pathway, whereas F5111 IC uses both pathways. Furthermore, F5111 IC, but not control IC, induced the association of human CD25 and CCR7 in human CD25-expressing 293T cells (Figure 6C). Overall, these IC studies reveal that engineered IL-2 formulations that direct signaling toward Tregs can also engage the Gαi/o-dependent non-canonical signaling and the association of human CD25 and CCR7 in the absence of anti-CD25 antibodies.

Amelioration of EAE by mPC61

To investigate the effects of engaging this alternative IL-2 signaling pathway *in vivo*, we administered murinized effector-incompetent mPC61, described in Figure 4, to mice undergoing EAE, a model autoimmune disease. Consistent with previous reports,[46] injection of rPC61 profoundly reduced Treg numbers. In peripheral blood, Tregs decreased from 6.9% ± 1.06% (mean ± SEM) to 3.1% ± 0.7% of CD4 cells 8 days after rPC61 administration (p = 0.0005) (Figure S5A). Similar degrees of depletion were observed in spleen and lymph nodes (Figure S5B). By contrast, mPC61 caused a slight transitory decrease in peripheral blood Tregs, but by day 8, Tregs in peripheral blood, lymph nodes, or spleen (Figure S5) were not reduced or increased by mPC61 administration, confirming previous work with a rat effector-incompetent PC61.[47] These results confirmed that mPC61 does not deplete nor expand Tregs and that it can be used to analyze the effect of ligating CD25 with this antibody *in vivo*.

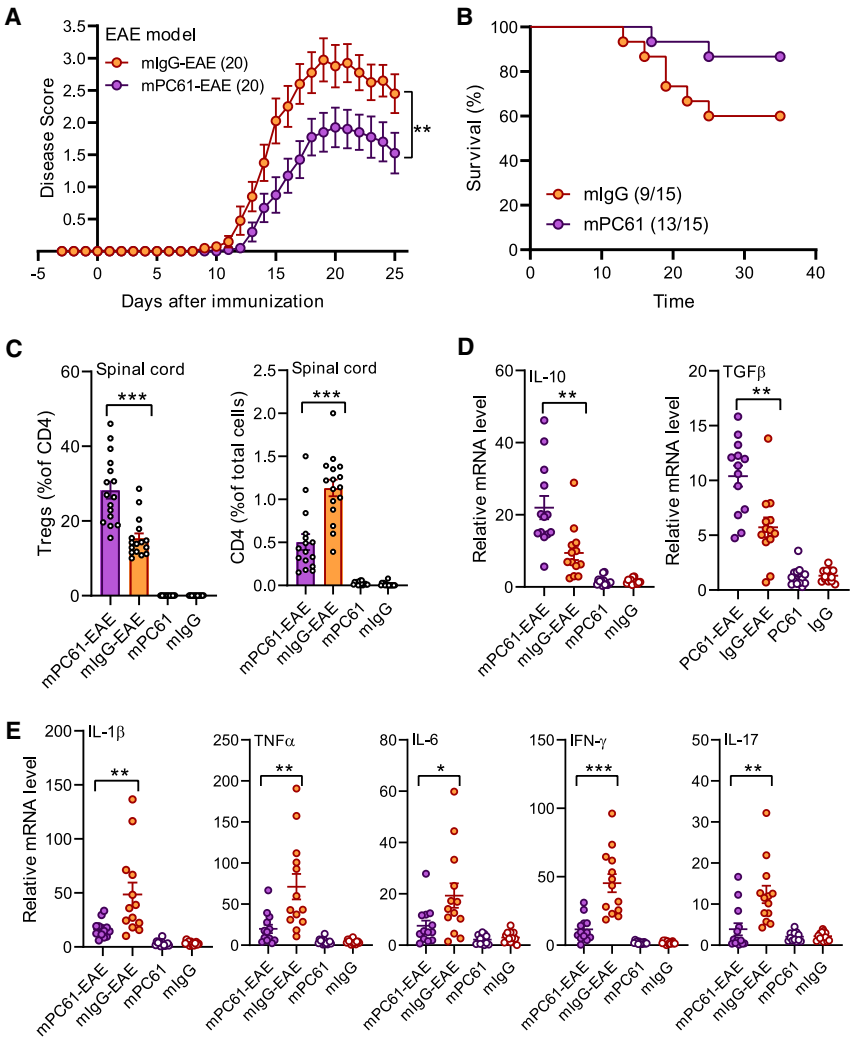

Figure 7. PC61 ameliorates EAE

EAE was induced on day 0 by immunization with MOG_{35-55} in complete Freund's adjuvant. Mice were treated with 10 mg/kg mPC61 or mIgG control on days −3, −2, −1, 2, 3, and 4 (n = 5–8 mice per group).

(A and B) Disease score (A) and survival rate (B) of mice with EAE treated with mPC61 or mIgG control. Data represent mean ± SEM (n = 20 in A or 15 in B). Two-way ANOVA with Bonferroni post-test.

(C) The percentage of GFP^+ Tregs in $CD4^+$ T cells (left) and $CD4^+$ T cells in total cells (right) in the spinal cords of mice at day 22 after MOG immunization. Data represent mean ± SEM (n = 16). One-way ANOVA with Bonferroni post-test.

(D and E) Expression of IL-10 and TGF-β (D) or IL-1β, TNF-α IL-6, IFN-γ, and IL-17A (E) mRNA in the spinal cords of mice at day 22 after MOG immunization. Results are normalized to GAPDH. Data represent mean ± SEM (n = 13). One-way ANOVA with Bonferroni post-test. NS, not significant; *p < 0.05; **p < 0.01; ***p < 0.001.

Because Tregs can suppress T cell-mediated autoimmune diseases,[46,48] we tested whether mPC61 could inhibit myelin oligodendrocyte glycoprotein (MOG_{35-55})[43]-induced EAE, a model of multiple sclerosis (Figure S6A). As expected, IgG control-treated *Foxp3*^{GFP} mice developed severe disease by 15 days after MOG/complete Freund's adjuvant (CFA) injection (Figure 7A) and exhibited reduced survival ~40% mice died by day 25 (Figure 7B). In dramatic contrast to the parent rPC61, which exacerbates EAE,[46] mPC61 treatment reduced EAE clinical manifestations and led to a trend toward ($p < 0.1$) increased survival (Figures 7A, 7B, and S6B). This amelioration of clinical disease was associated with increased relative abundance (Figure 7C) of GFP^+ Tregs and of mRNA encoding IL-10 and TGF-β mRNA in spinal cords of PC61-injected EAE mice. The reduced EAE symptomatology in mPC61-treated EAE mice was associated with a marked reduction in histologic $CD3^+$ T cell numbers and demyelination (Figure S6B) and was confirmed by reduced total CD4 cell numbers (Figure 7C) and an abundance of injurious cytokine mRNAs such as IL-1β and TNF-α (Figure 7E) in their spinal cords. Thus, mPC61 suppressed EAE associated with increased Tregs and their products in a target tissue, the spinal cord.

We utilized experimental colitis induced by dextran sulfate sodium (DSS) to assess whether the effect of mPC61 is generalizable to other models of inflammation. As in EAE, administration of mPC61 increased the relative abundance (Figure S7B) of GFP^+ Tregs and of mRNA encoding IL-10 and TGF-β mRNA (Figure S7C) in lamina propria of DSS-treated mice associated with a reduction in abundance of injurious cytokine mRNAs such as IL-1β and TNF-α (Figure S7D). Therefore, the capacity of mPC61 to modulate the presence of Tregs at the site of inflammatory tissue injury is potentially generalizable.

DISCUSSION

The α subunit of the IL-2 receptor (CD25) was discovered 40 years ago,[18] and seminal studies have established that CD25 participates in IL-2 signaling by forming a complex with the βγ subunits of the IL-2 receptor to activate intracellular JAKs and to shape immune responses.[1] Here, we report that CD25 bound to IL-2 can also form a complex with a chemokine receptor, and we elucidate a signaling pathway through which this interaction can boost $CD4^+CD25^{Hi}Foxp3^+$Treg function. Using an antibody to CD25 that enforces IL-2 signaling via the chemokine receptor pathway, we establish that this alternative IL-2 signaling pathway promotes the suppressive activity of Tregs and ameliorates murine EAE. A major IL-2-binding element of tissues, HS, and engineered versions of IL-2 (e.g., F5111 IC) can bias signaling toward this alternative pathway as well. Since the F5111 antibody within F5111 IC sterically blocks IL-2

engagement of the βγ IL-2 receptor,[6] our findings suggest that IL-2 variants with impaired βγ interaction may preferentially activate the alternative Gαi/o-dependent pathway, offering an opportunity for IL-2 signaling intervention. Moreover, the capacity of this alternative IL-2 signaling pathway to promote Tregs' suppressive function can enhance the maintenance of Treg abundance and function in tissues and can be exploited to blunt autoimmunity.

In addition to its canonical role in presenting IL-2 to the βγ subunits, CD25 can enable IL-2 signaling via chemokine receptors. PC61 is an allosteric inhibitor of IL-2 binding to CD25,[21] and thus its capacity to promote an IL-2-dependent signaling pathway appears paradoxical. Our studies reveal that PC61 induces a ternary complex containing CD25, IL-2, and CCR7 (Figures 6E and 6F) and that IL-2 binding to CD25 is required for complex formation. We also find that in the presence of PC61, IL-2 association with CD25 requires CCR7 (Figure 5F). These data suggest that the formation of this quaternary complex is enabled by the cooperative effects of IL-2 binding to both CD25 and CCR7, analogous to the stabilization of IL-2 binding in the trimeric αβγ high-affinity IL-2 receptor.[1] PTX ADP ribosylates Gαi, disrupting its association with GPCR. Dissociation of G proteins reduces GPCR affinity for ligands.[49] Our finding that PTX blocks the PC61-induced CD25/CCR7 association (Figures 5D and 5F) suggests that PC61-CD25 presents IL-2 to CCR7 as an authentic ligand. IL-2 is remarkably conformationally labile,[50] a property that accounts for the ability of certain anti-IL2 antibodies to bias signaling to Tregs[51] and for the capacity of CD25 to dramatically increase the affinity of IL2 for the CD122 β subunit.[52] Thus, we suggest that the binding of PC61 to CD25 can result in an altered conformation of bound IL-2 that favors its association with chemokine receptors.

As noted above, tissue-associated IL-2 is bound to glycosaminoglycans, in particular HS.[23,41] Our finding that HS-bound IL-2 can engage this alternative signaling pathway suggests that this pathway may play a role in Treg trafficking and maintenance. Indeed, elegant studies revealed that transgenic mice bearing visceral adipose tissue-specific T cell receptors can increase the abundance of Tregs, but not of Tconvs, in visceral fat.[53] Integrin activation plays an important role in maintenance of T cells in tissue niches.[15,54] Our data (Figure 6A) suggest that HS-bound IL-2, by preferentially activating Treg integrins via the non-canonical pathway, can help account for the selective enrichment of adipose tissue-specific transgenic Tregs versus Tconvs in visceral fat. Because non-canonical IL-2 signaling is promoted by monoclonal antibodies or components of the extracellular matrix, we suggest the acronym M-directed alternative cytokine signaling (MACS) for convenience (Figure 6D). Notably, IL-2 is a member of a family of 6 cytokines that have distinct α subunits and that signal through a common γ_c subunit,[55] raising the possibility that MACS involving other cytokines might also engage unexpected signaling receptors. Thus, we show that HS, antibodies against IL-2, or anti-CD25 can direct IL-2 to CCR7 to trigger a MACS pathway that enhances Treg function.

IL-2 MACS can impact therapeutic approaches to modification of IL-2 signaling and Treg function. Anti-CD25 antibodies that directly compete with IL-2 have been extensively developed for transplant reduction and autoimmunity; however, the adverse effects of such antibodies on Tregs and resulting autoimmune diseases have limited their use.[19,20] Conversely, anti-CD25 antibodies that do not block IL-2 binding and are optimized for antibody-dependent cellular cytotoxicity have been developed to deplete intra-tumoral Tregs, thereby augmenting immunotherapy.[22] Our data suggest a property of certain anti-CD25 antibodies is to redirect IL-2 to chemokine receptors as an alternative to the βγ signaling receptors. When such antibodies are engineered to block effector functions that mediate Treg clearance, they can inhibit EAE and increase the relative abundance of Tregs at the site of tissue injury. Our data also reveal that engineered IL-2 constructs, such as an IC, can engage IL-2 MACS. An IC, formed from human IL-2 and a human antibody, can drive the association of human CD25 with CCR7 (Figure 6C), showing that the human orthologs of IL-2, anti-IL-2 antibody, CD25, and CCR7 can form the complex that mediates MACS. Our data (Figure 1A and 1B) show that PC61 can stimulate Tregs but not naive Tconvs. That said, PC61 also induces Gi-dependent integrin activation in murine CD25-expressing Jurkat T cells (Figure S2), suggesting that the IL-2 MACS pathway can alter the function of other $CD25^{Hi}$ cells especially because it can utilize chemokine receptors other than CCR7 (Figure 4B). That said, we found that PC61 did not increase the differentiation of activated $CD8^+$ T cells into interferon γ (IFN-γ)-expressing effector T cells (Figure S8), indicating that the net biological effects of this pathway will depend on cellular context. Thus, the work reported here reveals that efforts to engineer IL-2 signaling should consider the potential role of MACS in both favorable and adverse therapeutic outcomes.

Limitations of this study

The study shows that an anti-CD25 can induce a complex of CD25, IL-2, and a chemokine receptor that triggers a signaling pathway that activates Treg integrins, can promote suppression, and can ameliorate murine EAE. There are limitations of this work that will require future study to fully explore its biological and potential therapeutic impact.

(1) Most of the work was performed with murine CD25 and IL-2. Although we show that a fully human F5111 IC can promote human CD25-CCR7 association, future work will be required to identify anti-human CD25 antibodies that can mimic the effects of PC61 on human Tregs.
(2) Murinized effector-incompetent PC61 (mPC61) ameliorated murine EAE, and this effect could be due PC61 interaction with another CD25-expressing cell rather than with Tregs. Importantly, the protective effect of mPC61 is absent in rPC61, which depletes Tregs and exacerbates EAE,[46] indicating that protection requires the presence of Tregs.
(3) We show that PC61-bound CD25 forms a complex with IL-2 and CCR7, but we have not established the order of interaction, i.e., does the IL-2 bind directly to the CCR7?
(4) We show that CD25 can be induced to form an IL-2-dependent complex with CCR7 that generates Gi-dependent signaling in Tregs; however, we also show it can operate in other CD25-expressing cells. The biological

effects of this mode of IL-2 signaling on these cells will require future study; however, here, we show that it does not promote increased frequency of IFN-γ-expressing activated $CD8^+$ T cells.

STAR★METHODS

Detailed methods are provided in the online version of this paper and include the following:

- KEY RESOURCES TABLE
- RESOURCE AVAILABILITY
  - Lead contact
  - Materials availability
  - Data and code availability
- EXPERIMENTAL MODEL AND STUDY PARTICIPANT DETAILS
  - Mouse strains
  - Mouse EAE
  - Mouse colitis model
  - Cell culture
- METHOD DETAILS
  - Cell lines and plasmids
  - Duolink Proximity Ligase Assay (PLA)
  - Flow cytometry
  - Tregs suppression assays
  - Enzyme-linked immunosorbent assay (ELISA)
  - STAT5 phosphorylation
  - mRNA purification, Real-time quantitative PCR (qPCR) analyses
  - siRNA transfection
  - Immunohistochemistry
  - Co-immunoprecipitation
  - Histology
- QUANTIFICATION AND STATISTICAL ANALYSIS

SUPPLEMENTAL INFORMATION

Supplemental information can be found online at https://doi.org/10.1016/j.celrep.2023.112996.

ACKNOWLEDGMENTS

This work was principally supported by a grant from the National Institutes of Health, HL-129947 (M.H.G.). Additional support was from HL-151433 (M.H.G. and M.A.L.-R.); EB029455 (J.B.S.); the Crohn's & Colitis Foundation Career Development Award 902590 (H.S.); HL145454 (Z.F.); the European Union's Horizon 2020 Framework Program research and innovation program Marie Skłodowska-Curie Actions grant 841428 (F.L.); and the Juvenile Diabetes Research Foundation 1-INO-2020-923-A-N to J.B.S. D.V. is the recipient of an ARCS® Foundation Metro-Washington Chapter Scholar award and a National Science Foundation Graduate Research Fellowship Program award.

AUTHOR CONTRIBUTIONS

H.S. and M.H.G. conceived the study, designed experiments, analyzed data, and wrote the manuscript. H.L., H.S., M.A.L.-R., J.A., M.F.d.L., and F.L. designed and executed experiments, analyzed data, and wrote the manuscript. J.B.S. and D.V. provided critical reagents. A.R.G. and J.T.C. provided critical conceptual input. Q.D. and W.M. designed and performed experiments. H.S., H.L., M.A.L.-R., J.A., F.L., J.T.C., J.B.S., and M.H.G. edited the manuscript.

DECLARATION OF INTERESTS

The authors declare no competing interests.

Received: September 7, 2022
Revised: April 18, 2023
Accepted: August 2, 2023
Published: August 21, 2023

REFERENCES

1. Ross, S.H., and Cantrell, D.A. (2018). Signaling and Function of Interleukin-2 in T Lymphocytes. Annu. Rev. Immunol. *36*, 411–433. https://doi.org/10.1146/annurev-immunol-042617-053352.
2. Sakaguchi, S., Yamaguchi, T., Nomura, T., and Ono, M. (2008). Regulatory T cells and immune tolerance. Cell *133*, 775–787. https://doi.org/10.1016/j.cell.2008.05.009.
3. Zhang, X., Olsen, N., and Zheng, S.G. (2020). The progress and prospect of regulatory T cells in autoimmune diseases. J. Autoimmun. *111*, 102461. https://doi.org/10.1016/j.jaut.2020.102461.
4. Romano, M., Fanelli, G., Albany, C.J., Giganti, G., and Lombardi, G. (2019). Past, Present, and Future of Regulatory T Cell Therapy in Transplantation and Autoimmunity. Front. Immunol. *10*, 43. https://doi.org/10.3389/fimmu.2019.00043.
5. Boyman, O., Kovar, M., Rubinstein, M.P., Surh, C.D., and Sprent, J. (2006). Selective stimulation of T cell subsets with antibody-cytokine immune complexes. Science *311*, 1924–1927. https://doi.org/10.1126/science.1122927.
6. Trotta, E., Bessette, P.H., Silveria, S.L., Ely, L.K., Jude, K.M., Le, D.T., Holst, C.R., Coyle, A., Potempa, M., Lanier, L.L., et al. (2018). A human anti-IL-2 antibody that potentiates regulatory T cells by a structure-based mechanism. Nat. Med. *24*, 1005–1014.
7. Khoryati, L., Pham, M.N., Sherve, M., Kumari, S., Cook, K., Pearson, J., Bogdani, M., Campbell, D.J., and Gavin, M.A. (2020). An IL-2 mutein engineered to promote expansion of regulatory T cells arrests ongoing autoimmunity in mice. Sci. Immunol. *5*, eaba5264.
8. Pilat, N., and Sprent, J. (2020). Treg Therapies Revisited: Tolerance Beyond Deletion. Front. Immunol. *11*, 622810. https://doi.org/10.3389/fimmu.2020.622810.
9. Klann, J.E., Kim, S.H., Remedios, K.A., He, Z., Metz, P.J., Lopez, J., Tysl, T., Olvera, J.G., Ablack, J.N., Cantor, J.M., et al. (2018). Integrin Activation Controls Regulatory T Cell-Mediated Peripheral Tolerance. J. Immunol. *200*, 4012–4023. https://doi.org/10.4049/jimmunol.1800112.
10. Sun, H., Lagarrigue, F., Wang, H., Fan, Z., Lopez-Ramirez, M.A., Chang, J.T., and Ginsberg, M.H. (2021). Distinct integrin activation pathways for effector and regulatory T cell trafficking and function. J. Exp. Med. *218*, e20201524. https://doi.org/10.1084/jem.20201524.
11. Sun, H., Lagarrigue, F., Gingras, A.R., Fan, Z., Ley, K., and Ginsberg, M.H. (2018). Transmission of integrin beta7 transmembrane domain topology enables gut lymphoid tissue development. J. Cell Biol. *217*, 1453–1465. https://doi.org/10.1083/jcb.201707055.
12. Hogg, N., Patzak, I., and Willenbrock, F. (2011). The insider's guide to leukocyte integrin signalling and function. Nat. Rev. Immunol. *11*, 416–426. https://doi.org/10.1038/nri2986.
13. Tadokoro, S., Shattil, S.J., Eto, K., Tai, V., Liddington, R.C., de Pereda, J.M., Ginsberg, M.H., and Calderwood, D.A. (2003). Talin binding to integrin beta tails: a final common step in integrin activation. Science *302*, 103–106. https://doi.org/10.1126/science.1086652.
14. Simonson, W.T.N., Franco, S.J., and Huttenlocher, A. (2006). Talin1 regulates TCR-mediated LFA-1 function. J. Immunol. *177*, 7707–7714.
15. Su, W., Wynne, J., Pinheiro, E.M., Strazza, M., Mor, A., Montenont, E., Berger, J., Paul, D.S., Bergmeier, W., Gertler, F.B., and Philips, M.R. (2015). Rap1 and its effector RIAM are required for lymphocyte trafficking. Blood *126*, 2695–2703. https://doi.org/10.1182/blood-2015-05-644104.

16. Stefanini, L., and Bergmeier, W. (2019). RAP GTPases and platelet integrin signaling. Platelets *30*, 41–47. https://doi.org/10.1080/09537104.2018.1476681.

17. Lagarrigue, F., Tan, B., Du, Q., Fan, Z., Lopez-Ramirez, M.A., Gingras, A.R., Wang, H., Qi, W., and Sun, H. (2022). Direct Binding of Rap1 to Talin1 and to MRL Proteins Promotes Integrin Activation in CD4(+) T Cells. J. Immunol. *208*, 1378–1388.

18. Leonard, W.J., Depper, J.M., Uchiyama, T., Smith, K.A., Waldmann, T.A., and Greene, W.C. (1982). A monoclonal antibody that appears to recognize the receptor for human T-cell growth factor; partial characterization of the receptor. Nature *300*, 267–269. https://doi.org/10.1038/300267a0.

19. Rech, A.J., Mick, R., Martin, S., Recio, A., Aqui, N.A., Powell, D.J., Jr., Colligon, T.A., Trosko, J.A., Leinbach, L.I., Pletcher, C.H., et al. (2012). CD25 blockade depletes and selectively reprograms regulatory T cells in concert with immunotherapy in cancer patients. Sci. Transl. Med. *4*, 134ra62. https://doi.org/10.1126/scitranslmed.3003330.

20. Stork, L., Brück, W., von Gottberg, P., Pulkowski, U., Kirsten, F., Glatzel, M., Rauer, S., Scheibe, F., Radbruch, H., Hammer, E., et al. (2019). Severe meningo-/encephalitis after daclizumab therapy for multiple sclerosis. Mult. Scler. *25*, 1618–1632. https://doi.org/10.1177/1352458518819098.

21. Moreau, J.L., Nabholz, M., Diamantstein, T., Malek, T., Shevach, E., and Thèze, J. (1987). Monoclonal antibodies identify three epitope clusters on the mouse p55 subunit of the interleukin 2 receptor: relationship to the interleukin 2-binding site. Eur. J. Immunol. *17*, 929–935. https://doi.org/10.1002/eji.1830170706.

22. Solomon, I., Amann, M., Goubier, A., Arce Vargas, F., Zervas, D., Qing, C., Henry, J.Y., Ghorani, E., Akarca, A.U., Marafioti, T., et al. (2020). CD25-T(reg)-depleting antibodies preserving IL-2 signaling on effector T cells enhance effector activation and antitumor immunity. Nat. Can. (Ott.) *1*, 1153–1166.

23. Wrenshall, L.E., and Platt, J.L. (1999). Regulation of T cell homeostasis by heparan sulfate-bound IL-2. J. Immunol. *163*, 3793–3800.

24. Kashiwakura, Y., Kojima, H., Kanno, Y., Hashiguchi, M., and Kobata, T. (2020). Heparin affects the induction of regulatory T cells independent of anti-coagulant activity and suppresses allogeneic immune responses. Clin. Exp. Immunol. *202*, 119–135. https://doi.org/10.1111/cei.13480.

25. Koliesnik, I.O., Kuipers, H.F., Medina, C.O., Zihsler, S., Liu, D., Van Belleghem, J.D., and Bollyky, P.L. (2020). The Heparan Sulfate Mimetic PG545 Modulates T Cell Responses and Prevents Delayed-Type Hypersensitivity. Front. Immunol. *11*, 132. https://doi.org/10.3389/fimmu.2020.00132.

26. Ortega, G., Robb, R.J., Shevach, E.M., and Malek, T.R. (1984). The murine IL 2 receptor. I. Monoclonal antibodies that define distinct functional epitopes on activated T cells and react with activated B cells. J. Immunol. *133*, 1970–1975.

27. Lee, H.S., Lim, C.J., Puzon-McLaughlin, W., Shattil, S.J., and Ginsberg, M.H. (2009). RIAM activates integrins by linking talin to ras GTPase membrane-targeting sequences. J. Biol. Chem. *284*, 5119–5127. https://doi.org/10.1074/jbc.M807117200.

28. Wilkinson, D.S., Ghosh, D., Nickle, R.A., Moorman, C.D., and Mannie, M.D. (2017). Partial CD25 Antagonism Enables Dominance of Antigen-Inducible CD25(high) FOXP3(+) Regulatory T Cells As a Basis for a Regulatory T Cell-Based Adoptive Immunotherapy. Front. Immunol. *8*, 1782. https://doi.org/10.3389/fimmu.2017.01782.

29. Sakaguchi, S., Mikami, N., Wing, J.B., Tanaka, A., Ichiyama, K., and Ohkura, N. (2020). Regulatory T Cells and Human Disease. Annu. Rev. Immunol. *38*, 541–566. https://doi.org/10.1146/annurev-immunol-042718-041717.

30. Yuan, X., Dong, Y., Tsurushita, N., Tso, J.Y., and Fu, W. (2018). CD122 blockade restores immunological tolerance in autoimmune type 1 diabetes via multiple mechanisms. JCI insight *3*, e96600. https://doi.org/10.1172/jci.insight.96600.

31. Burgdorf, C., Schäfer, U., Richardt, G., and Kurz, T. (2010). U73122, an aminosteroid phospholipase C inhibitor, is a potent inhibitor of cardiac phospholipase D by a PIP2-dependent mechanism. J. Cardiovasc. Pharmacol. *55*, 555–559. https://doi.org/10.1097/FJC.0b013e3181d8bec5.

32. Kang, M.S., Jung, S.Y., Jung, K.M., Kim, S.K., Ahn, K.H., and Kim, D.K. (2008). D609, an inhibitor of phosphatidylcholine-specific phospholipase C, inhibits group IV cytosolic phospholipase A2. Mol. Cell. *26*, 481–485.

33. Young, L.H., Balin, B.J., and Weis, M.T. (2005). Go 6983: a fast acting protein kinase C inhibitor that attenuates myocardial ischemia/reperfusion injury. Cardiovasc. Drug Rev. *23*, 255–272. https://doi.org/10.1111/j.1527-3466.2005.tb00170.x.

34. Wang, N., Hao, H.S., Li, C.Y., Zhao, Y.H., Wang, H.Y., Yan, C.L., Du, W.H., Wang, D., Liu, Y., Pang, Y.W., et al. (2017). Calcium ion regulation by BAPTA-AM and ruthenium red improved the fertilisation capacity and developmental ability of vitrified bovine oocytes. Sci. Rep. *7*, 10652. https://doi.org/10.1038/s41598-017-10907-9.

35. Cai, Y., Stafford, L.J., Bryan, B.A., Mitchell, D., and Liu, M. (2005). G-protein-activated phospholipase C-beta, new partners for cell polarity proteins Par3 and Par6. Oncogene *24*, 4293–4300. https://doi.org/10.1038/sj.onc.1208593.

36. Mangmool, S., and Kurose, H. (2011). G(i/o) protein-dependent and -independent actions of Pertussis Toxin (PTX). Toxins *3*, 884–899. https://doi.org/10.3390/toxins3070884.

37. Lee, J.H., Kang, S.G., and Kim, C.H. (2007). FoxP3+ T cells undergo conventional first switch to lymphoid tissue homing receptors in thymus but accelerated second switch to nonlymphoid tissue homing receptors in secondary lymphoid tissues. J. Immunol. *178*, 301–311. https://doi.org/10.4049/jimmunol.178.1.301.

38. Clynes, R.A., Towers, T.L., Presta, L.G., and Ravetch, J.V. (2000). Inhibitory Fc receptors modulate in vivo cytotoxicity against tumor targets. Nat. Med. *6*, 443–446. https://doi.org/10.1038/74704.

39. Abrams, J.S., Roncarolo, M.G., Yssel, H., Andersson, U., Gleich, G.J., and Silver, J.E. (1992). Strategies of anti-cytokine monoclonal antibody development: immunoassay of IL-10 and IL-5 in clinical samples. Immunol. Rev. *127*, 5–24. https://doi.org/10.1111/j.1600-065x.1992.tb01406.x.

40. Pawelec, G., Borowitz, A., Krammer, P.H., and Wernet, P. (1982). Constitutive interleukin 2 production by the JURKAT human leukemic T cell line. Eur. J. Immunol. *12*, 387–392. https://doi.org/10.1002/eji.1830120506.

41. Wrenshall, L.E., Platt, J.L., Stevens, E.T., Wight, T.N., and Miller, J.D. (2003). Propagation and control of T cell responses by heparan sulfate-bound IL-2. J. Immunol. *170*, 5470–5474.

42. Wegener, K.L., Partridge, A.W., Han, J., Pickford, A.R., Liddington, R.C., Ginsberg, M.H., and Campbell, I.D. (2007). Structural basis of integrin activation by talin. Cell *128*, 171–182. https://doi.org/10.1016/j.cell.2006.10.048.

43. Webster, K.E., Walters, S., Kohler, R.E., Mrkvan, T., Boyman, O., Surh, C.D., Grey, S.T., and Sprent, J. (2009). In vivo expansion of T reg cells with IL-2-mAb complexes: induction of resistance to EAE and long-term acceptance of islet allografts without immunosuppression. J. Exp. Med. *206*, 751–760. https://doi.org/10.1084/jem.20082824.

44. Spangler, J.B., Trotta, E., Tomala, J., Peck, A., Young, T.A., Savvides, C.S., Silveria, S., Votavova, P., Salafsky, J., Pande, V.S., et al. (2018). Engineering a Single-Agent Cytokine/Antibody Fusion That Selectively Expands Regulatory T Cells for Autoimmune Disease Therapy. J. Immunol. *201*, 2094–2106. https://doi.org/10.4049/jimmunol.1800578.

45. VanDyke, D., Iglesias, M., Tomala, J., Young, A., Smith, J., Perry, J.A., Gebara, E., Cross, A.R., Cheung, L.S., Dykema, A.G., et al. (2022). Engineered human cytokine/antibody fusion proteins expand regulatory T cells and confer autoimmune disease protection. Preprint at bioRxiv. https://doi.org/10.1001/2022.05.29.493918.

46. Stephens, L.A., Gray, D., and Anderton, S.M. (2005). CD4+CD25+ regulatory T cells limit the risk of autoimmune disease arising from T cell receptor crossreactivity. Proc. Natl. Acad. Sci. USA *102*, 17418–17423. https://doi.org/10.1073/pnas.0507454102.

47. Hayes, E.T., Hagan, C.E., Khoryati, L., Gavin, M.A., and Campbell, D.J. (2020). Regulatory T Cells Maintain Selective Access to IL-2 and Immune Homeostasis despite Substantially Reduced CD25 Function. J. Immunol. *205*, 2667–2678. https://doi.org/10.4049/jimmunol.1901520.

48. Wood, K.J., and Sakaguchi, S. (2003). Regulatory T cells in transplantation tolerance. Nat. Rev. Immunol. *3*, 199–210. https://doi.org/10.1038/nri1027.

49. Staus, D.P., Strachan, R.T., Manglik, A., Pani, B., Kahsai, A.W., Kim, T.H., Wingler, L.M., Ahn, S., Chatterjee, A., Masoudi, A., et al. (2016). Allosteric nanobodies reveal the dynamic range and diverse mechanisms of G-protein-coupled receptor activation. Nature *535*, 448–452. https://doi.org/10.1038/nature18636.

50. De Paula, V.S., Jude, K.M., Nerli, S., Glassman, C.R., Garcia, K.C., and Sgourakis, N.G. (2020). Interleukin-2 druggability is modulated by global conformational transitions controlled by a helical capping switch. Proc. Natl. Acad. Sci. USA *117*, 7183–7192. https://doi.org/10.1073/pnas.2000419117.

51. Spangler, J.B., Tomala, J., Luca, V.C., Jude, K.M., Dong, S., Ring, A.M., Votavova, P., Pepper, M., Kovar, M., and Garcia, K.C. (2015). Antibodies to Interleukin-2 Elicit Selective T Cell Subset Potentiation through Distinct Conformational Mechanisms. Immunity *42*, 815–825. https://doi.org/10.1016/j.immuni.2015.04.015.

52. Wang, X., Rickert, M., and Garcia, K.C. (2005). Structure of the quaternary complex of interleukin-2 with its alpha, beta, and gammac receptors. Science *310*, 1159–1163. https://doi.org/10.1126/science.1117893.

53. Li, C., DiSpirito, J.R., Zemmour, D., Spallanzani, R.G., Kuswanto, W., Benoist, C., and Mathis, D. (2018). TCR Transgenic Mice Reveal Stepwise, Multi-site Acquisition of the Distinctive Fat-Treg Phenotype. Cell *174*, 285–299.e12. https://doi.org/10.1016/j.cell.2018.05.004.

54. Sun, H., Fan, Z., Gingras, A.R., Lopez-Ramirez, M.A., Ginsberg, M.H., and Ley, K. (2020). A Flexible Kink in the Transmembrane Domain Impairs β2 Integrin Extension and Cell Arrest from Rolling. J. Leukoc. Biol. *107*, 175–183.

55. Yang, H., Kureshi, R., and Spangler, J.B. (2019). Structural Basis for Signaling Through Shared Common γ Chain Cytokines. Adv. Exp. Med. Biol. *1172*, 1–19. https://doi.org/10.1007/978-981-13-9367-9_1.

56. Klapproth, S., Sperandio, M., Pinheiro, E.M., Prünster, M., Soehnlein, O., Gertler, F.B., Fässler, R., and Moser, M. (2015). Loss of the Rap1 effector RIAM results in leukocyte adhesion deficiency due to impaired beta2 integrin function in mice. Blood *126*, 2704–2712. https://doi.org/10.1182/blood-2015-05-647453.

57. Petrich, B.G., Marchese, P., Ruggeri, Z.M., Spiess, S., Weichert, R.A.M., Ye, F., Tiedt, R., Skoda, R.C., Monkley, S.J., Critchley, D.R., and Ginsberg, M.H. (2007). Talin is required for integrin-mediated platelet function in hemostasis and thrombosis. J. Exp. Med. *204*, 3103–3111. https://doi.org/10.1084/jem.20071800.

58. Stefanini, L., Ye, F., Snider, A.K., Sarabakhsh, K., Piatt, R., Paul, D.S., Bergmeier, W., and Petrich, B.G. (2014). A talin mutant that impairs talin-integrin binding in platelets decelerates alphaIIbbeta3 activation without pathological bleeding. Blood *123*, 2722–2731. https://doi.org/10.1182/blood-2013-12-543363.

59. Hogquist, K.A., Jameson, S.C., Heath, W.R., Howard, J.L., Bevan, M.J., and Carbone, F.R. (1994). T cell receptor antagonist peptides induce positive selection. Cell *76*, 17–27.

60. Lee, P.P., Fitzpatrick, D.R., Beard, C., Jessup, H.K., Lehar, S., Makar, K.W., Pérez-Melgosa, M., Sweetser, M.T., Schlissel, M.S., Nguyen, S., et al. (2001). A critical role for Dnmt1 and DNA methylation in T cell development, function, and survival. Immunity *15*, 763–774.

61. Rubtsov, Y.P., Rasmussen, J.P., Chi, E.Y., Fontenot, J., Castelli, L., Ye, X., Treuting, P., Siewe, L., Roers, A., Henderson, W.R., Jr., et al. (2008). Regulatory T cell-derived interleukin-10 limits inflammation at environmental interfaces. Immunity *28*, 546–558. https://doi.org/10.1016/j.immuni.2008.02.017.

62. Fontenot, J.D., Dooley, J.L., Farr, A.G., and Rudensky, A.Y. (2005). Developmental regulation of Foxp3 expression during ontogeny. J. Exp. Med. *202*, 901–906.

63. Law, A.L., Vehlow, A., Kotini, M., Dodgson, L., Soong, D., Theveneau, E., Bodo, C., Taylor, E., Navarro, C., Perera, U., et al. (2013). Lamellipodin and the Scar/WAVE complex cooperate to promote cell migration in vivo. J. Cell Biol. *203*, 673–689. https://doi.org/10.1083/jcb.201304051.

64. Berlin, C., Bargatze, R.F., Campbell, J.J., von Andrian, U.H., Szabo, M.C., Hasslen, S.R., Nelson, R.D., Berg, E.L., Erlandsen, S.L., and Butcher, E.C. (1995). alpha 4 integrins mediate lymphocyte attachment and rolling under physiologic flow. Cell *80*, 413–422.

65. Sun, H., Liu, J., Zheng, Y., Pan, Y., Zhang, K., and Chen, J. (2014). Distinct chemokine signaling regulates integrin ligand specificity to dictate tissue-specific lymphocyte homing. Dev. Cell *30*, 61–70. https://doi.org/10.1016/j.devcel.2014.05.002.

66. Lyons, J.A., Ramsbottom, M.J., and Cross, A.H. (2002). Critical role of antigen-specific antibody in experimental autoimmune encephalomyelitis induced by recombinant myelin oligodendrocyte glycoprotein. Eur. J. Immunol. *32*, 1905–1913. https://doi.org/10.1002/1521-4141(200207)32:7<1905::AID-IMMU1905>3.0.CO;2-L.

67. Rodrigues, D.H., Vilela, M.d.C., Barcelos, L.d.S., Pinho, V., Teixeira, M.M., and Teixeira, A.L. (2010). Absence of PI3Kgamma leads to increased leukocyte apoptosis and diminished severity of experimental autoimmune encephalomyelitis. J. Neuroimmunol. *222*, 90–94. https://doi.org/10.1016/j.jneuroim.2010.02.016.

STAR★METHODS

KEY RESOURCES TABLE

REAGENT or RESOURCE	SOURCE	IDENTIFIER
Antibodies		
InVivoMAb rat IgG1 Isotype control, anti-trinitrophenol (Control of PC61)	BioXcell	BE0290;RRID:AB_2687813
Recombinant Anti-Integrin beta 7 antibody [EPR1357] (ab108926)	Abcam	ab108926;RRID:AB_10862762
Alexa Fluor® 647 Mouse Anti-STAT5 (pY694) Clone 47/STAT5 (pY694) (RUO)	BD	612599;RRID:AB_399882
APC anti-human CD184 (CXCR4) Antibody	Biolegend	306509;RRID:AB_314615
Ultra-LEAF™ Purified anti-mouse CD122 (IL-2Rβ) Antibody	Biolegend	123224;RRID:AB_2810373
Alexa Fluor® 647 anti-human IgG Fc Antibody	Biolegend	410714;RRID:AB_2728444
PE anti-STAT5 Phospho (Tyr694) Antibody	Biolegend	936904;RRID:AB_2832913
Purified anti-mouse CD25 Recombinant Antibody	Biolegend	162102;RRID:AB_2890727
Purified anti-mouse CD25 Antibody-3C7	Biolegend	101902;RRID:AB_312845
Purified Rat IgG2b, κ Isotype Ctrl Antibody (RTK4530)	Biolegend	400602;RRID:AB_326546
APC anti-mouse CD197 (CCR7) Antibody	Biolegend	120107;RRID:AB_389233
APC anti-human CD197 (CCR7) Antibody	Biolegend	353213;RRID:AB_10915474
PE anti-mouse/rat/human FOXP3 Antibody, clone 150D	Biolegend	320008;RRID:AB_492980
Alexa Fluor® 647 anti-mouse/rat/human FOXP3 Antibody	Biolegend	320014;RRID:AB_439750
APC anti-mouse CD4 Antibody (GK1.5)	Biolegend	100412;RRID:AB_312697
APC Rat IgG2b, κ Isotype Ctrl Antibody (RTK4530)	Biolegend	400612;RRID:AB_326556
Purified anti-mouse CD25 Antibody-7D4	Biolegend	154202;RRID:AB_2716173
Purified Rat IgM, κ Isotype Ctrl (RTK2118)	Biolegend	400802;RRID:AB_326578
Purified anti-mouse CD3ε Antibody (145-2C11)	Biolegend	100301;RRID:AB_312666
Purified anti-mouse CD28 Antibody (37.51)	Biolegend	102102;RRID:AB_312867
Purified anti-mouse IL-2 Antibody (JES6-1A12)	Biolegend	503701;RRID:AB_315291
Alexa Fluor® 647 anti-mouse IL-10 Antibody (JES5-16E3)	Biolegend	505014;RRID:AB_493511
Alexa Fluor® 647 Rat IgG2b, κ Isotype Ctrl Antibody (RTK4530)	Biolegend	400626;RRID:AB_389343
APC anti-mouse LAP (TGF-β1) Antibody (TW7-16B4)	Biolegend	141406;RRID:AB_10898159
APC Mouse IgG1, κ Isotype Ctrl Antibody (MOPC-21)	Biolegend	400119;RRID:AB_2888687
LEAF™ Purified anti-mouse IL-2 Antibody_JES6-5H4 Neut	Biolegend	503812;RRID:AB_315306
Alexa Fluor® 647 Goat anti-mouse IgG (minimal x-reactivity) Antibody	Biolegend	405322;RRID:AB_2563045
Biotin anti-mouse CD25 Antibody (PC61)	Biolegend	102004;RRID:AB_312853
Purified anti-mouse CD3 Antibody (17A2)	Biolegend	100238;RRID:AB_2561487
Alexa Fluor® 488 anti-mouse CD25 Antibody (PC61)	Biolegend	102017;RRID:AB_493333
InvivomAb MOPC-21 mIgG1 isotype control	BioXcell	BE0083;RRID:AB_1107784
InVivoMAb anti-mouse CD25 (IL-2Rα), PC-61.5.3	BioXcell	BE0012;RRID:AB_1107619
Phospho-STAT5 (Tyr694) (C71E5) Rabbit mAb (PE Conjugate) #5387	Cell Signaling Technology	5387;RRID:AB_2797611
Goat polyclonal anti-CCR7	Thermo-Fisher	PA1-21613;RRID:AB_2072904
Alexa Fluor® 647 AffiniPure F(ab')₂ Fragment Donkey Anti-Human IgG	Jackson ImmunoResearch	709-606-098;RRID:AB_2340580
Mouse monoclonal anti-HA (12CA5)	Lab stock	
Donkey anti-goat IgG, IRDye 680RD	Licor	926-68074;RRID:AB_10956736
Biotin-Mouse CD25/IL-2R alpha	R&Dsystems	BAF2438;RRID:AB_416766
Streptividin-DyLight™ 800	Rockland	S000-45

(*Continued on next page*)

Continued

REAGENT or RESOURCE	SOURCE	IDENTIFIER
Monoclonal Anti-Talin antibody produced in mouse (8d4)	Sigma	T3287;RRID:AB_477572
Goat anti-Rabbit IgG (H + L) Highly Cross-Adsorbed Secondary Antibody, Alexa Fluor 647	ThermoScietific	A21245;RRID:AB_141775
Bacterial and virus strains		
Bacteria: *E.coli* Stellar™ Competent Cells	Takara	Cat# 636766
Chemicals, peptides, and recombinant proteins		
Lipofectamine™ 3000	Invitrogen	Cat# L3000015
Protein G Resin	GenScript	L00209
Perm Buffer III	BD	558050
Recombinant Mouse ICAM-1-Fc Chimera (carrier-free)	Biolegend	553006
Recombinant Human VCAM-1-Fc Chimera (carrier-free)	Biolegend	553706
Recombinant Mouse IL-2 (carrier-free)	Biolegend	575406
MojoSort™ Buffer (5X)	Biolegend	480017
Recombinant Mouse CCL21 (6CKine) (carrier-free)	Biolegend	586404
Recombinant Mouse CXCL12 (SDF-1α) (carrier-free)	Biolegend	578704
16% Paraformaldehyde (formaldehyde) aqueous solution	Electron Microscopy Science	15710
MOG35-55/CFA Emulsion PTX	Hooke	EK-2110
100 mL-EDTA (0.5 M), pH 8.0	Life Technologies Corporation	AM9260G
Goat Anti-Rat IgG (H + L) MicroBeads (quote70261717-00)	Miltenyi	130-048-502
Recombinant Mouse MAdCAM-1 Fc Chimera Protein, CF	R&D systems	993-MC-050
DuoLink *InSitu* Wash Buffer, Brightfield	Sigma	DUO82047-4L
Heparin sodium salt from porcine intestinal mucosa	Sigma	H3149-50KU
Heparan sulfate sodium salt from bovine kidney	Sigma	H7640-1MG
Phorbol 12-myristate 13-acetate, phorbol ester, PMA	Sigma	P1585
Dimethyl sulfoxide (DMSO)	Sigma	D2650
BAPTA-AM	Sigma	A1076
Pertussis toxin	Sigma	P7208
FluoroMyelin™ Red Fluorescent Myelin Stain	Sigma	F34652
Bovine Albumin Fraction V (7.5% solution)	Thermo Fisher	15260037
HBSS, Calcium, Magnesium, no phenol red	Thermo Fisher	14025134
Media, Cell Culture, Gibco, Opti-MEM I Reduced Serum Medium	Thermo Fisher	31985062
GeneAmp dNTP Blend (2.5 mM ea)	Thermo Fisher Scientific	N8080260
FreeStyle™ 293 Expression Medium	ThermoScietific	12338018
U 73122, >98%, Tocris, 10mg,	Tocris	126810
D609, greater than 98%, Tocris, 10mg	Tocris	143710
Go 6983	Tocris	22851
LY 294002 hydrochloride	Tocris	11305
Baricitinib	Tocris	7222
Critical commercial assays		
eBioscience™ Foxp3/Transcription Factor Staining Buffer Set	Ebiosciences	00-5523-00
ExpiFectamine™ 293 Transfection Kit	Thermo Fisher	A14524
Transcription Factor Phospho Buffer Set	BD	565575
MojoSort™ Mouse CD4 T cell Isolation Kit	Biolegend	480033
MojoSort™ Mouse CD4 Naive T cell Isolation Kit	Biolegend	480040
LEGEND MAX™ Mouse Latent TGF-β ELISA Kit	Biolegend	433007
LEGEND MAX™ Mouse IL-10 ELISA Kit	Biolegend	431417
Duolink® flowPLA Mouse/Rabbit Starter Kit - Far Red	DUO94104-1KT	Sigma
Quick-RNA MiniPrep Kit Zymo Research Kit, 50 Preps/Unit	Genesee Scientific	11–327

(*Continued on next page*)

Continued

REAGENT or RESOURCE	SOURCE	IDENTIFIER
Direct-zol RNA MiniPrep (50μg)	Genesee Scientific	11–330
ToxinSensor Chromogenic LAL Endotoxin Assay Kit	Genscript	L00350C
PrimeScript 1st strand cDNA synthesis kit	Takara	6110B
Experimental models: Cell lines		
Expi293f Cells - 1mL	Thermo Fisher	A14527;RRID:CVCL_D615
Jurkat T cells	ATCC	TIB-152;RRID:CVCL_0367
293T cells	Takara	632180;
Experimental models: Organisms/strains		
B6.SJL-Ptprca Pepcb/BoyJ/Ly5.1 mice	The Jackson Laboratories	Stock No: 002014; RRID:IMSR_JAX:002014
C57BL/6J	The Jackson Laboratories	Stock No: 000664; RRID: IMSR_JAX:000664
C.Cg-Foxp3tm2Tch/J/Foxp3EGFP mice	The Jackson Laboratories	Stock No: 006769; RRID: IMSR_JAX:006769
Rap1a/bfl/fl, Foxp3Cre mice	Previous study,[9–11]	Grown in house
Tln1fl/fl, Foxp3Cre mice	Previous study,[9–11]	Grown in house
Apbb1ip,Raph1fl/fl, Foxp3Cre mice	Previous study,[9–11]	Grown in house
Oligonucleotides		
ON-TARGETplus Human CCR7 siRNA	Dharmacon (Horizon Discovery)	L-005454-00-0005
ON-TARGETplus Human CXCR4 siRNA	Dharmacon (Horizon Discovery)	L-005139-00-0005
siGENOME Non-Targeting siRNA Control Pool #1	Dharmacon (Horizon Discovery)	D-001206-13-20
Primers for mutagenesis, see method details	This paper	N/A
qPCR primers, see Table S1	This paper	N/A
Recombinant DNA		
Plasmid: pLVX-Het1	Clontech	635074
Plasmid: pMDLg/pRRE	Addgene	Plasmid #12251;RRID: Addgene_12251
Plasmid: pRSV-Rev	Addgene	Plasmid #12253;RRID: Addgene_12253
Plasmid: pCMV-VSV-G	Addgene	Plasmid #8454;RRID: Addgene_8454
Plasmid: HP150 (pCDNA3.1_mPC61_VL)	This paper	N/A
Plasmid: HP151 (pCDNA3.1_D265A_VH)	This paper	N/A
Plasmid: HP172 (pLVX-Het-1_mCD25)	This paper	N/A
Plasmid: pcDNA3.1(−)-HA-mouse CD25	This paper	N/A
Plasmid: pLVXHet1-HA-mouse CD25	This paper	N/A
Plasmid: pLVXHet1-HA-mouse CD25(2E)	This paper	N/A
Software and algorithms		
GraphPad Prism 8	Graphpad	Version 8
ImageJ		https://imagej.nih.gov/ij/

RESOURCE AVAILABILITY

Lead contact

Further information and requests for resources and reagents should be directed to and will be fulfilled by the Lead Contact, Dr. Mark Ginsberg (mhginsberg@health.ucsd.edu).

Materials availability

Plasmids and mouse models generated in this study will be available upon request.

Data and code availability

- All data reported in this paper will be shared by the lead contact upon request.
- This paper does not report original code.
- Any additional information required to reanalyze the data reported in this paper is available from the lead contact upon request.

EXPERIMENTAL MODEL AND STUDY PARTICIPANT DETAILS

Mouse strains

All animal experiments were approved by the Institutional Animal Care and Use Committee (IACUC) of the University of California, San Diego, and were conducted in accordance with federal regulations as well as institutional guidelines and regulations on animal studies. All mice were housed in specific pathogen-free conditions. C57BL/6 (CD45.1) and C57BL/6 (CD45.2) mice were from The Jackson Laboratory. *Apbb1ip*$^{fl/fl}$*Raph1*$^{fl/fl}$, *Tln1*$^{fl/fl}$, *Rap1a* $^{fl/fl}$*b* $^{fl/fl}$, *Rap1b* $^{fl/fl}$, *Foxp3*$^{Cre\text{-}YFP}$ and *Foxp3*^{GFP} mice have been described previously.[10,15,56–63] For experiments, 8-12-week-old mice were used. All injections of cells were performed during the light cycle. All experiments were performed by comparing mice with littermate controls. Mononuclear cells were isolated from mesenteric lymph node (MLN), Peyer's patch (PP), peripheral lymph node (PLN), spleen (SP) and colonic lamina propria as previously described.[64,65] Cell counting with immunofluorescence cytometry was performed using an Accuri C6 Plus and FACSCalibur (BD Biosciences).

Mouse EAE

The study was performed on *Foxp3*^{GFP} female mice of 10–13 weeks of age. The animals were housed in groups of three in a controlled 12 h light/12 h dark schedule, and free access to water and food until the beginning of the experiments. Animals were randomly assigned to one of the four groups: mPC61-treated EAE induction group, mIgG-treated EAE induction group, mPC61-treated control group (PBS), and mIgG-treated control group (PBS).

Immunization kits based on MOG35-55/CFA emulsion and Pertussis Toxin (PTX) (code EK-2110) were purchased from Hooke Laboratories, Inc, Lawrence, MA, USA, with the protocol being developed as indicated by the producer.[66] mPC61 or mIgG (200 μg/mouse) were daily injected into the *Foxp3*^{GFP} female mice by i.p. on day-3, day-2, day-1, day2, day 3 and day4. On day 0, the animals received initially the MOG35-55 antigen emulsion in two subcutaneous injections (0.1 mL/site) on the upper and lower back areas. At 2 h after the last antigen injection, the first PTX dose was injected intraperitoneally (150ng diluted in 0.1mL glycerol/PBS buffer). In the next day (day 1), the second PTX dose was injected intraperitoneally in the same concentration. Control animals received saline of the same volume. The animals were then followed for 40 days, with their motor dysfunction being scored by a blinded observer following EAE scoring guide[67]: 0 (no disease), 0.5 (distal limp tail, tip of the tail drops), 1 (normal gait, tail drops), 1.5 (hindlimb paresis, uncoordinated gait), 2 (uncoordinated gait with one hind paw dragging, tail limps), 2.5 (uncoordinated gait with both hind paws dragging, tail limps), 3 (hind paws paralyzed, weakness in forepaws), 3.5 (hind paws paralyzed, one forepaw paralyzed), 4 (hind paws paralyzed, both forepaws paralyzed), 4.5 (moribund), 5 (the mouse is only rolling or is found dead). After the beginning of the induction, all animals were fed with freshly prepared 2% agarose-glucose pellets. To assess the spinal cord, mice were euthanized on day 22 and spinal cords were isolated.

Mouse colitis model

In acute colitis experiments, *Foxp3*^{GFP} mice administered 2% (w/v) Dextran Sulfate Sodium (DSS) with a molecular weight of 36–50 kDa (MP Biomedicals, Irvine, CA) in drinking water for total of 7 days (days 0–7), followed by plain drinking water (days 8–16). The mice were intraperitoneally injected with mPC61 or control mouse IgG1 (100 μg/mouse) every 3 days. Mice were euthanized and colons were isolated on the last day of the observation for analysis.

Cell culture

$CD4^+CD25^-$ T cells were isolated from spleens of C57BL/6 (CD45.1) mice by magnetic separation using the $CD4^+$ T cell negative isolation kit (Biolegend) and cultured in RPMI-1640 medium supplemented with 10% FBS, non-essential amino acids, 1x Penicillin/Streptomycin, 2mM L-glutamine, and 5 μg/mL immobilized antibodies against CD3 (145-2C11, Biolegend) and CD28 (37.51, Biolegend), and IL-2 (6 ng/mL) for 5 days at 37°C. The Jurkat cells were cultured in RPMI-1640 medium supplemented with 10% FBS, non-essential amino acids, 1x Penicillin/Streptomycin, and 2mM L-glutamine at 37°C in a 5% CO2 incubator.

HEK293T cells were cultured in DMEM supplemented with 10% FBS, non-essential amino acids, 1x Penicillin/Streptomycin, and 2mM L-glutamine at 37°C in a 5% CO2 incubator.

METHOD DETAILS

Cell lines and plasmids

Jurkat cells that stably expressed mouse CD25 (mCD25) were generated by lentiviral transduction followed by selection with puromycin and cell sorting. mCD25-expressing lentiviral particles were prepared by cotransfection of pLVX-Het1-mCD25 with pMDLg/pRRE, pRSV-Rev, and pMD2.G in 293T cells. Supernatants containing lentiviral particles were collected. For lentiviral delivery, Jurkat

cells were grown to 80% confluence and then infected with pLVX-mCD25 containing lentiviral particles. Cells were then selected with puromycin (2 μg/mL) 72 h after infection.

For 293T cells, mammalian expression construct encoding HA-full-length mouse CD25 (HA-mCD25) were generated in pcDNA 3.1(−) with forward primer 5′-gatatctgcagaattatggagccacgcttgctgatgttggggtttctctcattaaccatagtacccagttgtcgggcatacccatacgat gttccagattacgctgaactgtgtctgtat-3′ and reverse primer 5′-ggtaccgagctcggatccctagatggttcttctgct-3′ and pLVX-Het1 with forward primer 5′- tatttccggtgaattcatggagccacgcttgctgatgttggggtttctctcattaaccatagtacccagttgtcgggcatacccatacgatgttccagattacgctgaact gtgtctgtat-3′ and reverse primer 5′-gtcatacgtaggatccctagatggttcttctgct-3'. HA-mouse CD25(2E, R57E-V62E, HA-mCD25(2E)) was produced by site directed mutagenesis with forward primer 5′-aagagaggtttccgagaactaaaggaattggaatatatgcgttgctta-3′ and reverse primer 5′- taagcaacgcatatattccaattcctttagttctcggaaacctctctt-3'.

293T cells transiently expressing HA-mCD25 and HA-mCD25(2E) were generated by Lipofectamine 3000 transfection (Invitrogen).

Duolink Proximity Ligase Assay (PLA)

Duolink Proximity Ligase Assay was conducted using Duolink PLA kit for flow cytometry with Far Red detection and Mouse/Rabbit probes (Millipore-Sigma, DUO94104). Briefly, CD4 T cells (1 x 10^7) isolated from *Foxp3*^{GFP} mice were stimulated with mPC61 or mIgG in 37°C for 30min, fixed, permeabilized, stained with rabbit anti-mouse CCR7 (Invitrogen A1-21613) overnight at 4°C. Secondary incubation anti-rabbit PLUS and anti-mouse MINUS probes, ligation, amplification and wash steps were completed in solution as directed by the manufacturer. The mean fluorescence intensity (MFI) of GFP$^+$ Tregs and GFP$^-$ Tconvs was quantified by flow cytometry analysis using an Accuri C6 Plus (BD Biosciences). The sample without CCR7 antibody was used as a negative control and observed fluorescence was subtracted from other conditions.

Flow cytometry

Cells isolated from mouse tissues or cell lines were washed and resuspended in PBS containing 0.1% BSA and stained with conjugated antibody for 30 min at 4°C. Then cells were washed twice before flow cytometry analysis using an Accuri C6 Plus (BD Biosciences). Data were analyzed using FlowJo 10.1 software.

For soluble ligand binding assay, 5×10^6 cells were washed and resuspended in HBSS containing 0.1% BSA and 1 mM Ca^{2+}/Mg^{2+}, prior to incubation with integrin ligands for 30 min at 37°C in presence with or without 100 nM PMA. Cells were then incubated with AlexFluor647-conjugated anti-human IgG (1:200) for 30 min at 4°C.

For intracellular detection of cytokines, splenocytes were stimulated *ex vivo* with PMA and ionomycin in the presence of brefeldin A and monensin for 6 h at 37°C; cells were fixed in 4% paraformaldehyde (Electron Microscopy Services) and permeabilized with the Foxp3 transcription factor fixation/permeabilization kit (eBioscience) prior to IL-10, TGF-β1 and Foxp3 staining.

For STAT5 staining, cells were fixed with Fix Buffer 1 (BD) and permeabilized with Perm buffer III (BD) after extracellular staining, for intracellular staining. Samples were analyzed with an Accuri C6 Plus (BD Biosciences). Data were then analyzed with FlowJo 10.1 software.

Tregs suppression assays

CD4$^+$CD25$^-$ T cells (Responder cells) were isolated from spleens of C57BL/6 (CD45.1) WT mice by magnetic separation using the CD4$^+$ T cell negative isolation kit (Biolegend); a biotin-conjugated anti-CD25 (PC61; Biolegend) Ab was included to deplete Tregs. GFP$^+$ Tregs from *Foxp3*^{GFP} mice or YFP$^+$ Tregs from were sorted with a FACSAria 2 (BD Biosciences). Responder cells were labeled with CFSE and cocultured with Tregs (8:1, 4:1, 2:1 and 1:1 ratios) stimulated with 5 μg/mL PC61 or IgG control in the presence of immobilized anti-CD3 mAb (145-2C11 clone, 5 μg/mL), anti-CD28 mAb (37.51 clone, 5 μg/mL), and IL-2 (6 ng/mL) for 5 days at 37°C. Division index was calculated by FlowJo v10.

For pre-treated Tregs, Tregs were treated with 5 μg/mL PC61 or IgG control for 30 min at 37°C, washed and cultured with responder cells in the presence of immobilized anti-CD3 mAb (145-2C11 clone, 5 μg/mL), anti-CD28 mAb (37.51 clone, 5 μg/mL), and IL-2 (6 ng/mL) for 5 days at 37°C.

For supernatant treatment, CD4$^+$ T cells were isolated from spleens of *Foxp3*^{GFP} mice by magnetic separation using the CD4$^+$ T cell negative isolation kit (Biolegend) and treated with 5 μg/mL PC61 or IgG control in the culture medium for 30 min at 37°C. Then the cells were washed and cultured at 37°C for 5 days. After that, the supernatants were collected and added into CFSE-labelled responder cells in the presence of immobilized anti-CD3 mAb (145-2C11 clone, 5 μg/mL), anti-CD28 mAb (37.51 clone, 5 μg/mL), and IL-2 (6 ng/mL) for 5 days at 37°C before analysis.

Enzyme-linked immunosorbent assay (ELISA)

To detect IL-10 and TGF-β, CD4$^+$ T cells were isolated from spleens of *Foxp3*^{GFP} mice by magnetic separation using the CD4$^+$ T cell negative isolation kit (Biolegend) and treated with 5 μg/mL PC61 or IgG control in the culture medium for 5 days at 37°C. Then the supernatants were collected and the IL-10 and TGF-β concentrations in the supernatant were measured by ELISA kit (Mouse IL-10: 431417; Mouse TGF-β: 433007; Biolegend) using the manufacturer's supplied standards and recommended protocol.

STAT5 phosphorylation

2 x 10^6 splenocytes from male *Foxp3*^{GFP} mice were plated in each well of a 96-well plate and incubated with mIL-2, PC61, IgG control, or mIL-2 plus baricitinib in PBS. Cells were stimulated for 15 min at 37°C and immediately fixed and permeabilized by the Transcription Factor Phospho Buffer Set (BD Biosciences). Cells were then washed twice with FACS buffer (PBS, pH 7.2, containing 0.1% BSA) and incubated with Alexa Fluor 647-conjugated anti-STAT5 pY694 (1:50, BD Biosciences) and PE-conjugated anti-Foxp3 (1:50, Biolegend) for 2 h at room temperature. Cells were then washed twice in FACS buffer, and mean fluorescence intensity (MFI) was determined on an Accuri 6 flow cytometer (BD Biosciences).

Dose-response curves were fitted to a logistic model, and EC50s were calculated using GraphPad Prism data analysis software after subtraction of the MFI of unstimulated cells and normalization to the maximum signal intensity. Triplicate measurements were made in each experiment and each experiment was independently replicated at least three times with similar results.

mRNA purification, Real-time quantitative PCR (qPCR) analyses

Total RNA was isolated from spinal cord or colon using tissue homogenizer (JXFSTPRP-24, ThunderSci) and TRIzol reagent according to the manufacturer's protocol (Thermo Fisher Scientific). For gene expression analysis, single-stranded cDNA was produced from 10 μg total RNA of colon using SuperScript III First-Strand synthesis and oligo-dT primers according to the manufacturer's protocol (Thermo Fisher Scientific). Kappa SybrFast qPCR kit (Kapa Biosystems) and thermal cycler (CFX96 Real-Time System; Bio-Rad) were used to determine the relative levels of the genes analyzed (primer sequences are shown in Table S1) according to the manufacturer's protocol. The $2^{-\Delta\Delta CT}$ method was used for analysis, and data were normalized to GAPDH.

siRNA transfection

siRNA pools that target human CCR7 or CXCR4, and non-targeting control siRNA pools were purchased from Dharmacon, Horizon Discovery. Jurkat cells were maintained at a density of 1 × 10^6 cell/ml and sub-cultured 24 h before transfection. For electroporation-based transfection, 5 × 10^6 cells were used per reaction in a 6-well plate. The cells were washed twice with 1× PBS and resuspended into 100 μL Nucleofector V-Kit with 50 μM siRNA. Then the cells/siRNA suspensions were transferred into cuvettes and electroporated by using the Nucleofector (Amexa, program T-001). Immediately after electroporation, 400 μL of the pre-equilibrated culture medium to the cuvette was added and transferred to a 6-well plate with 1.5 mL medium. 24 h post-transfection, the medium was changed with fresh medium; 48 h post-transfection, cells were subjected with a second round of siRNA transfection; and 24 h post-second siRNA transfection, the media were changed again. The cells were harvested for analysis 72 h post-second siRNA transfection.

Immunohistochemistry

Spinal cords were cryoprotected in 30% sucrose dissolved in PBS, Spinal cords were embedded and frozen in O.C.T compound (23-730-571; FischerScientific). Tissues were cut into 18-μm coronal sections onto Superfrost Plus slides (12-550-15; VWE International). Sections were blocked and permeabilized in a permeabilization solution (0.5% Triton X-100, 5% goat serum, 0.5% BSA, in PBS) for 2h and incubated in rat monoclonal antibody against CD3 (1:100; 17A2 clone; Biolegend) in PBS at room temperature overnight. Tissue sections were washed four times in PBS and incubated with suitable Alexa Fluor coupled secondary antibodies (1:300, ThermoFisher) in PBS for 1h at RT. FluoroMyelin Red was used to visualize myelin in spinal cords following the manufacturer's protocol (1:300, ThermoFisher). Cell nuclei were stained with DAPI and mounted with Fluoromount-G mounting medium (SouthernBiotech). The slides were viewed with a high-resolution SP8 confocal microscope (Leica Microsystems), and the images were captured with Leica application suite software (Leica Microsystems).

Co-immunoprecipitation

Cells were transfected by plasmids using lipofectamine 3000 (Invitrogen) and incubated for 24 h before lysis in NP-40 lysis buffer (50 mM Tris-HCl pH 7.4, 150 mM NaCl, 0.5% NP-40, 0.5mM $CaCl_2$, 0.5mM $MgCl_2$, 1μM calpeptin, protease inhibitor cocktail) on ice for 15 min. The lysate was centrifuged at 14,000 rpm at 4°C for 15 min and the detergent-solubilized cell lysate was immunoprecipitated using designated primary antibodies with protein G resin (GenScript) at 4°C overnight. Then, immune complexes were washed with the lysis buffer and recovered by boiling in SDS sample buffer before separation by SDS-PAGE gels. Proteins on the gel were transferred to nitrocellulose membrane and probed with indicated primary and secondary antibodies.

Histology

Frozen sections of 18-μm thickness were mounted on positively charged Superfrost Plus slides (12-550-15; VWE International). The mounted tissue was fixed in cold acetone (maintained at 4°C) for 10 min at RT. Sections were then air-dried for 1 min and stained in Hematoxylin (GHS232, MilliporeSigma) solution for 3 min. To eliminate the excess staining solution, sections were briefly rinsed in tap water and in acid alcohol for 30 s. After rinsing again in tap water, sections were immersed in Scott's solution for 30 s and counterstained in Eosin (HT10116, Millipore Sigma) solution for 5 min. Next, the slides were rinsed in tap water and dehydrated by serial immersion in a graded series of ethanol solutions (70%, 80%, 90% and 100%, v/v) for 10 s in each solution. Finally, slides were cleared in xylene for 2 min and mounted with coverslips using xylene-based mounting medium. Slides were viewed in a bright field microscope (Keyence) and images acquired using Keyence BZ-X800 software.

QUANTIFICATION AND STATISTICAL ANALYSIS

Statistical analysis was performed using PRISM software (version 8.00, GraphPad Software), and all datasets were checked for Gaussian normality distribution. Data analysis was performed using two-tailed t test, one-way ANOVA or two-way ANOVA followed by Bonferroni post-test as indicated in the Figure legends. The resulting p values are indicated as follows: NS: not significant, $p > 0.05$; *, $0.01 < p < 0.05$; **, $0.001 < p < 0.01$; ***, $p < 0.001$. Plotted data are the mean ± SEM of at least five independent experiments.